A Generalized Nonlinear Model for the Evolution of Low Frequency Freak Waves

Jonathan M Blackledge *

Abstract— **This paper presents a generalized model for simulating wavefields associated with the sea surface. This includes the case when 'freak waves' may occur through an effect compounded in the nonlinear (cubic) Schrödinger equation. After providing brief introductions to linear sea wave models, 'freak waves' and the linear and nonlinear Schrödinger equations, we present a unified model that provides for a piecewise continuous transition from a linear to a nonlinear state. This is based on introducing a fractional time derivative to develop a fractional nonlinear partial differential equation with a stochastic source function. In order to explore the characteristics of this equation, we consider a separation of variables approach in order to derive governing equations for the spatial and temporal behaviour.**

Models for the source function (which, in physical terms, describes the conversion of wind energy into wave energy) are also considered on a separable basis. With regard to the temporal characteristics, we provide a new model that is based on assuming Lévy processes for the time-dependent wind velocity informed by experimental data. We consider a spatial frequency model that is based on a generalization of Berman and Ornstein-Uhlenbeck processes. This provides a statistically self-affine source function which has a synergy with the Pierson-Moskowitz model for the spectral form of fully developed wind driven seas based on 'similarity theory'.

Having presented the source function models, solutions to the governing nonlinear wave equations are explored using a Green's function transformation under a low frequency bandwidth condition. Iterative methods of solution are then considered in three-dimensions and then in two-dimensions. Example results are presented based on considering a first order solution that is equivalent to the application of the Born approximation for the linear Schrödinger equation. The simulations provide evidence for the formation of freak waves being related to the fact that the wind force (as a function of time) is non-Gaussian distributed. Consequently, freak waves are more common than would be expected using Gaussian statistics.

Keywords: Nonlinear Schrödinger equation, Generalized model, Lévy statistics, Sea surface waves, Freak waves.

*Dublin Institute of Technology, Kevin Street, Dublin 8, Ireland; http://eleceng.dit.ie/blackledge; jonathan.blackledge@dit.ie; +35 31 402 4707.

1 Introduction

There are a number of aspects about the dynamical behaviour of the sea surface that are obvious. For example, the state of the sea can change radically from 'calm' to 'rough' and the height and wavelength of sea waves can vary significantly. In nearly all case, 'sea states' are determined by the interaction of the wind (in particular, the wind force, i.e. the rate of change of wind velocity) with the sea surface and as a general rule, greater 'wind energy' results in greater 'wave power'.

1.1 Linear Sea Wave Models

There are two principal measurable properties of sea surface waves: their height and period of oscillation. Real ocean waves do not generally occur at a single frequency but have a frequency distribution for which a range of linear models have been developed. For example, if $s(t)$ denotes the spectral density as a function of the wave period t in seconds, then, for a linear wave pattern, it can be shown that [1] and [2]

$$s(t) = \alpha t^3 \exp(-\beta t^4)$$

where α and β are given by

$$\alpha = 8.10 \times 10^{-3} \frac{g^2}{(2\pi)^4}$$

and

$$\beta = 0.74 \left(\frac{g}{2\pi v} \right)$$

respectively, v is the wind velocity measured 19.5m above still water and g is the acceleration due to gravity.

Models of this type are non-realistic for a number of reasons: (i) They do not take into account that wave states are non-stationary; (ii) there is no modelling of the connectivity between the wind velocity and wave energy; (iii) it is assumed that the wind velocity is constant and no statistical variability in wind velocity is taken into account; (iv) they assume that local wind conditions and swell are correlated and are thereby not capable of explaining the 'split spectra' phenomenon, for example, in which the spectrum of the wavefield consists of two distinct peaks.

Linear wave spectrum models assume that the distance over which the waves develop and the duration for which the wind blows are sufficient for the waves to achieve their maximum energy for the given wind speed. It is assumed that waves can be represented by sinusoidal forms. This relies on the following: (i) Waves vary in a regular way around an average wave height; (ii) there are no energy losses due to friction or turbulence, for example; (iii) the wave height is much smaller than the wavelength.

Linear models are used to predict wave height, at least on a statistical basis. These assume that wave height conforms to a Rayleigh distribution given by

$$P(h) = \frac{h}{\sigma^2} \exp\left(-\frac{h^2}{2\sigma^2}\right)$$

where h is the wave crest height and σ is the most probable wave height. The 'Significant Wave Height' (SWH) is then defined as the average of one third of the maximum wave height which, based on this Rayleigh distribution, is given by

$$\text{SWH} = 2.2\sigma$$

In high storm condition with significant wave heights $\sim$ 15m, this statistical model suggests that it is rare to obtain waves higher than 15m and that the probability of obtaining waves with heights of more than twice the SWH is of the order of 10^{-5}. This result is a direct consequence of assuming linear models for deep ocean surface wavefields and can not account for the existence of 'freak waves' that have been observed and measured with increasing regularity throughout the worlds oceans.

1.2 Freak Waves

Freak waves, e.g. [3], [4] [5] and [6], have been know about for many years but it is only relatively recently that experimental data has been obtained on their occurrence and research has been undertaken into their cause. A well known example of experimental evidence for freak waves is given in Figure 1 which is a signal of the wave height (in metres) as a function of time (in second) recorded on New year's Day, 1995, using a radar pulse-echo system setup on the *Draupner* oil rig on the North Sea off Norway [11], [12]. In this case, a freak wave of approximately 26m was measured.

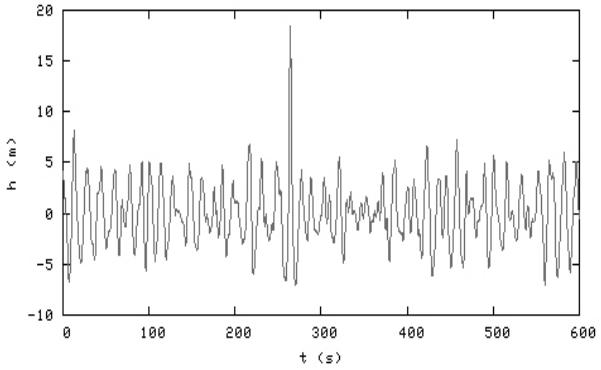

Figure 1: Wave height (in metres) as a function of time (in seconds) recorded on New year's Day, 1995, using a radar pulse-echo system setup on the *Draupner* oil rig in the North Sea off Norway.

The example given in Figure 1 is typical of freak waves generated in deep water that evolve in stormy conditions with high wind energies. A freak wave is not the same as a Tsunami that are mass displacement generated waves that propagate at high speed and are more or less unnoticeable in deep water, rising in wave height as they approach the shoreline. A freak wave is a spatially and temporally localized event that most frequently occurs far out at sea. Freak waves of up to 35m in height are much more common than probability theory would predict using a Rayleigh distribution for wave heights. They appear to occur in all of the world's oceans many times every year during a storm. This has called for a reexamination of the reasons for their existence, as well as reconsideration of the implications for ocean-going ship design [6] and wave energy conversion technology, e.g. [7], [8], [9] and [10].

There appear to be three principal categories of freak waves:

- **Walls of water** travelling up to 10km over the ocean surface before become extinct.
- **Three sisters** which are groups of three waves.
- **Single, giant storm waves** that build up to more than four times the average height of storm waves and then collapse over a relatively small time scale (in seconds).

These wave types are only three of a range of freak wave phenomena that have yet to be fully classified. It is clear that, whatever the range and diversity of freak waves, their existence can not be explained using linear wave models. One of the most common models used to explain these effects is the Nonlinear Schrödinder equation which is the focus of this paper. However, there are other physical reasons for the generation of freak waves which include the following:

- **Diffraction Effects.** Like optical and acoustic waves, sea surface waves can be diffracted producing a diffraction pattern that is related to the angle of incidence and the shape of the coat and/or seabed. In some cases, the diffraction pattern produces a focus where a collection of relatively small waves coherently combine in phase to produce a freak wave. The basic physics of this effect is the same as in optics accept in terms of scale where the wavelength of the wavefield is relatively large and the frequency spectrum is very low.
- **Current Focusing.** If storm force waves are driven together from opposite directions as opposing 'current' then the wavelength of the waves are shortened causing an increase in wave height. Oncoming wave trains are then 'compressed' together into a freak wave.

It is known that freak waves occur in deep water when diffraction effects can not be the cause and current focusing is weak. In this case, the freak wave is taken to be the result of a nonlinear effect in which the energy of many randomly generated waves is combined into a single wave front which continues to grow until collapsing under its own weight.

With regard to nonlinear effects the cubic nonlinear Schrödinger equation appears to be valid in deep water conditions. This equation forms the central theme of the work presented and developed in this paper which includes three principal contributions:

- unification of linear and nonlinear models;
- a model for random wave motion as a function of time based on experimental data with regard to wind velocity;
- a model for the low frequency spatial distribution of sea surface wave.

Freak wave are considered to be part of a wave spectrum and in this sense, freak waves are not 'freak' but part of a normal wave generation process, albeit a rare extremity. In this paper, the extremity is shown to be related to the non-Gaussian statistics that a wind force exhibits. As wind blows over the ocean, energy is transferred to the sea surface generating a wave spectrum. We introduce a model for the transfer of this energy which is inclusive of extreme cases that cause the nonlinear effect to become a dominant component of the unified model that is considered. This compliments the theories of instability mechanisms for the generation and growth of wind waves, e.g. [17], [18].

2 Linear and Nonlinear Schrödinger Equations

The Schrödinger equation is a differential representation of the (non-relativistic) energy equation

$$E = \frac{p^2}{2m} + V \tag{1}$$

which states that the energy E of a particle of mass m and with momentum p is the sum of the kinetic energy $p^2/(2m)$ and the potential energy denoted by V which is taken to be a function of space $\mathbf{r} \equiv (x, y, z)$. The basic postulates of quantum mechanics are that $E = \hbar\omega$ and $\mathbf{p} = \hbar\mathbf{k}$ where ω is the angular frequency, $\mathbf{k}$ is the wavenumber vector and where $h = 2\pi\hbar$ is Planck's constant. Noting that $p \equiv |\,\mathbf{p}\,|$ and $k \equiv |\,\mathbf{k}\,|$, we have

$$\frac{E}{p} = \frac{\omega}{k} = c$$

where c is the velocity of a wave with angular frequency ω and wavelength $2\pi/k$. Since, (1) can be written as

$$p = \sqrt{2m(E - V)}$$

it follows that

$$c^2 = \frac{E^2}{2m(E - V)}$$

and the basic wave equation

$$\left(\nabla^2 - \frac{1}{c^2}\frac{\partial^2}{\partial t^2}\right)\Psi(\mathbf{r}, t) = 0, \quad \nabla^2 \equiv \frac{\partial^2}{\partial x^2} + \frac{\partial^2}{\partial y^2} + \frac{\partial^2}{\partial z^2}$$

for a wave function Ψ becomes

$$\left[\nabla^2 - \frac{2m(E - V)}{E^2}\frac{\partial^2}{\partial t^2}\right]\Psi(\mathbf{r}, t) = 0 \tag{2}$$

If we consider the wave function $\Psi(\mathbf{r}, t)$ in terms of its temporal Fourier transform $\psi(\mathbf{r}, \omega)$ where

$$\psi(\mathbf{r}, \omega) = \int_{-\infty}^{\infty} \Psi(\mathbf{r}, t)\exp(-i\omega t)dt$$

and

$$\Psi(\mathbf{r},t)=\frac{1}{2\pi}\int_{-\infty}^{\infty}\psi(\mathbf{r},\omega)\exp(i\omega t)d\omega$$

then, noting that $E=\hbar\omega$, (2) is reduced to the form

$$i\hbar\psi(\mathbf{r},\omega)=\frac{-\hbar^2}{2m}\nabla^2\psi(\mathbf{r},\omega)+V\psi(\mathbf{r},\omega)$$

Inverse Fourier transforming, we then obtain Schödinger's equation

$$i\hbar\partial_t\Psi(\mathbf{r},t)=\frac{-\hbar^2}{2m}\nabla^2\Psi(\mathbf{r},\omega)+V\Psi(\mathbf{r},t) \tag{3}$$

where

$$\partial_t\equiv\frac{\partial}{\partial t}$$

Here, the wave function Ψ is taken to describe the wave-type behaviour of a non-relativistic particle of mass m such as an electron. In the context of this equation, we are typically concerned with the problem of of solving the equation for Ψ given V or, with regard to the inverse scattering problem, solving for V given ψ. The wave-field Ψ is a 'matter wave' as it describes the behaviour of non-relativistic particles of matter on the atomic scale. However, only the intensity $\mid\Psi\mid^2$ is a measurable quantity which is interpreted in terms of the probability density function associated with the position of a particle in space. The probability of finding a particle described by the wave function Ψ in the finite volume element $d^3\mathbf{r}$ around a point at $\mathbf{r}$ is $\mid\Psi(\mathbf{r},k)\mid^2\ d^3\mathbf{r}$ which yields the normalization condition

$$\int_{-\infty}^{\infty}\mid\Psi(\mathbf{r},t)\mid^2\ d^3\mathbf{r}=1$$

However, ignoring a particle interpretation of the Schrödinger, $\mid\Psi\mid^2$ is a measure of the energy of the wavefield Ψ. Moreover, this is the only measure that can be detected experimentally in quantum mechanics.

In scattering theory, we are interested in how an incident wave function Ψ_0 interacts with a potential in order to calculate the characteristic scattering cross-section $\mid\Psi\mid^2$ given Ψ_0 and V. In this case, the potential is taken to be independent of the wave function and the problem is inherently linear.

2.1 The Nonlinear Schrödinger Equation

The nonlinear Schrödinger equation is concerned with problems associated with a potential V that is a function of Ψ, i.e. when we consider the case where the interaction of a wave is with some characteristic of the wave itself, e.g. [13], [14], [15] and [16]. An example of this arises when $V=\mid\Psi\mid^2$ and for normalized units (i.e. $\hbar=1$ and $m=1/2$), Schrödinger's equation becomes

$$(\nabla^2+i\partial_t)\Psi=\kappa\mid\Psi\mid^2\Psi \tag{4}$$

where κ is a constant coefficient. This equation is known as the cubic nonlinear Schrödinger equation as its nonlinear behaviour is characterized by the cube of the wave functions amplitude. It represents a model in which a wave interacts with its own energy $\mid\Psi\mid^2$ where κ determines the strength of the 'self-interaction' and may be generalized to be $\pm\kappa$. In scattering theory, the wave is taken to be interacting and scattering with itself. This is an example of a 'wave-wave' interaction as opposed to a 'wave-particle' interaction when V represents the potential associated with a 'particle' which is entirely independent of the wave function Ψ. The cubic nonlinear Schrödinger equation is completely integrable in one dimension, mass-critical in two-dimensions, and energy critical in four dimensions.

2.2 Other Nonlinear Schrödinger Equations

Although (4) is the most commonly quoted nonlinear form of Schrödinger's equation, it is just one of a wide class of such equations. Writing (4) in the form

$$(\nabla^2+i\partial_t)\Psi=\kappa Q(\psi)$$

the following Table 1 classifies different forms of the Nonlinear Schrödinger (NLS) equation in terms of Q. In addition the NLS equations given in Table 1, higher-order NLS equations involve the Laplacian being replaced by a higher power Laplacian. For fractional powers, the Reisz definition of a fractional n-dimensional Lapacian is used, i.e. for $p>1$

$$\nabla^{2p}\Psi(\mathbf{r},t)=-\frac{1}{(2\pi)^n}\int_{-\infty}^{\infty}\mid\mathbf{k}\mid^{2p}\widetilde{\Psi}(\mathbf{k},t)\exp(i\mathbf{k}\cdot\mathbf{r})d^n\mathbf{k}$$

Examples of such classes include: (i) the infinite hierarchy of commuting flows arising from the completely integrable cubic NLS equation on $\mathbb{R}^1$; (ii) the elliptic case of the Zakharov-Schulman system [19]. Further examples of NLS equation-type systems include the differential NLS equations where, working in $\mathbb{R}^1$,

$$Q=i\partial_x(\mid\Psi\mid^2\Psi)$$

Moreover NLS equations can include additional terms describing a source s or scattering potential V so that we have

$$(\nabla^2+i\partial_t)\Psi=\kappa Q(\psi)+V\Psi+s$$

Table 1: Classification of NLS Equations

Q	Type of NLS Equation	Comment
Ψ^2	Qudratic	Mass critical in four dimensions
$\mid \Psi \mid^2 \Psi$	Cubic	Basic form of the NLS Equation
$\mid \Psi \mid^{2n}$, $n = 1, 2, 3, ...$	Integer Power Law	Generalized NLS Equation
$\mid \Psi \mid^{p-1}, p > 1$	Non-integer Power Law	Semilinear NLS Equation
$\mid \Psi \mid^{\frac{4}{n}}, \mathbf{r} \in \mathbb{R}^n$	$\mathbb{R}^2$-Critical	Solutions are scale invariant in $\mathbb{R}^2$

which leads to many physically interesting problems, a summary of which lies beyond the scope of this paper. However, the cubic NLS equation occurs naturally as a model equation for many different physical contexts, especially in dispersive, weakly non-linear perturbations of a plane wave. For instance, it arises as a model for Bose-Einstein condensates [20].

In this paper we focus on the cubic NLS equation with a source function s given by

$$(\nabla^2 + i\partial_t)\Psi = \kappa \mid \Psi(\mathbf{r}, t) \mid^2 \Psi(\mathbf{r}, t) + s(\mathbf{r}, t)$$

as a model for fully nonlinear sea surface waves working primarily in $\mathbb{R}^2$. However, it is important to note that, like the Schrödinger equation itself, i.e. equation (3), all classes of the NLS equation are phenomenological in origin. Equation (3) is a direct consequence of Planck's and De Broglie's postulates $E = \hbar\omega$ and $\mathbf{p} = \hbar\mathbf{k}$, respectively, that are justified experimentally. The validity of results that the Schrödinger equation predicts and which can be confirmed experimentally are ultimately the only justification for this equation. Thus, the Schrödinger equation is one of the most intriguing equations of physics in that it cannot be derived and its solution Ψ cannot be measured directly. Yet, to-date, it provides one of the most accurate models for characterizing the nature of matter. In light of the above comments, the material presented in this paper is ultimately based on a phenomenological model.

2.3 Example Analytical Solution to the NLS Equation

Certain analytic solutions exist to the NLS equation, specifically for the one-dimensional case. For example, consider the cubic case when

$$i\partial_t \Psi(x,t) + \partial_x^2 \Psi(x,t) + 2\Psi(x,t) \mid \Psi(x,t) \mid^2 = 0$$

This equation has two types of 'soliton solutions' associated with a group of wave functions. The first is the 'soliton' solution given by [21]

$$\Psi(x,t) = \frac{\exp(it)}{\cosh(x)}$$

This solution describes an envelope that does not change its form with time. The second class of solutions are of the form [22], [23]

$$\Psi(x,t) = \exp(2it)\frac{\cosh(\Omega t - 2i\theta) - \cos(\theta)\cos(px)}{\cosh(\Omega t) - \cos(\theta)\cos(px)}$$

where

$$p = 2\sin\theta \quad \text{and} \quad \Omega = 2\sin(2\theta)$$

The amplitude is periodic in time with frequency Ω and for real θ, the solution tends to an unperturbed plane wave as $\mid x \mid \to \infty$. For $\mid x \mid \to 0$, the solution describes a wave that begins as a modulated plane wave and evolves into one or several peaks that 'extract energy' from the surrounding peaks. The peak values for $\Psi(x,t)$ are twice the amplitude of the unperturbed value of the wave function and for imaginary θ, $\Psi(x,t)$ becomes a space period wave that tends to an unperturbed plane wave as $\mid t \mid \to \infty$, [25]. The maximum value of the peak amplitude is approximately three times the unperturbed value (depending on θ). For the limiting case, when $\theta \to 0$, we can consider the algebraic solution [24]

$$\Psi(x,t) = \exp(2it)\left(1 - \frac{4(4+4it)}{1+4x^2+16t^2}\right)$$

It is this aspect of the available analytical solutions that has been considered responsible for the generation of deep water freak. The freak waves observed in the numerical simulations based on the NLS equation can be approximately modelled by this algebraic solution [26].

3 Generalized Model

The Cubic NLS equation is the lowest order NLS equation that has proved to be successful in modelling deep ocean nonlinear sea surface waves, [27], [28]. However, it does not explain how a sea surface wavefield pattern can transform from a linear to a nonlinear state. It is

not physically significant to consider a nonlinear model for one (high wind energy) state and a linear model for another (low wind energy) state without attempting to explain the nature of the transition from one state to another. This paper is concerned with solving this problem by introducing a model that combines both linear and nonlinear models for sea waves. Thus, we consider the following problem: Let the linear model for low energy sea waves be given by (for normalized unit $c = 1$)

$$(\nabla^2 - \partial_t^2)\Psi(\mathbf{r}, t) = -s(\mathbf{r}, t)$$

where s is some source function and let the nonlinear model for high energy sea waves be given by the Cubic NLS equation

$$(\nabla^2 + i\partial_t)\Psi(\mathbf{r}, t) = -\kappa \mid \Psi(\mathbf{r}, t) \mid^2 \Psi(\mathbf{r}, t)$$

Find a generalized model that combines these two equation into one equation. In order to solve this problem, we need to include a fractional derivative of time $\partial_t^q, q \in [1, 2]$ in order to take into account the transition form a linear wave model characterized by a second derivative in time to a nonlinear model characterized by a first order derivative. An equation that achieves this goal is

$$\left(\nabla^2 + i^q \partial_t^q\right) \Psi(\mathbf{r}, t) = -\kappa \mid \Psi(\mathbf{r}, t) \mid^2 \Psi(\mathbf{r}, t) - s(\mathbf{r}, t) \quad (5)$$

where $q \in [1, 2]$ and $\kappa = (2 - q)$.

Then

$$\left(\nabla^2 + i\partial_t\right) \Psi(\mathbf{r}, t) = - \mid \Psi(\mathbf{r}, t) \mid^2 \Psi(\mathbf{r}, t) - s(\mathbf{r}, t), \quad q = 1$$

and

$$\left(\nabla^2 - \partial_t^2\right) \Psi(\mathbf{r}, t) = -s(\mathbf{r}, t), \quad q = 2$$

Here the 'Fourier Dimension' q (so called because we use the Fourier transform to define ∂_t^q) represents a variable parameter that can be used to adjust the degree of nonlinearity of the equation. It provides control on the dominance or 'strength' of the nonlinear term $\mid \Psi \mid^2 \Psi$ with respect to the source term $s(x, t)$. In proposing this model, we have introduced a fractional time derivative and the analysis that follows focuses attention on the temporal and spatial behaviour of the wave function Ψ as a result of introducing a fractional partial differential equation of this type.

4 Low Frequency Green's Function Transformation

We consider a general solution to (5) based on the Green's function transformation. This transformation is considered in the infinite domain so that the surface integral is zero (homogeneous boundary conditions). We investigate the Green's functions solutions under a low frequency bandwidth condition which provides a route to simplification that is compatible with a low frequency sea surface wavefield.

Taking the Fourier transform of (5) and using the product theorem, i.e.

$$\mid \Psi(\mathbf{r}, t) \mid^2 \Psi(\mathbf{r}, t) \leftrightarrow (2\pi)^2 \psi(\mathbf{r}, \omega) \odot_\omega \psi^*(\mathbf{r}, \omega) \otimes_\omega \psi(\mathbf{r}, \omega),$$

we obtain

$$\left(\nabla^2 + \omega^q\right) \psi(\mathbf{r}, \omega)$$

$$= -\kappa(2\pi)^2 [\psi(\mathbf{r}, \omega) \odot_\omega \psi^*(\mathbf{r}, \omega)] \otimes_\omega \psi(\mathbf{r}, \omega) - S(\mathbf{r}, \omega)$$

where

$$\psi(\mathbf{r}, \omega) = \int_{-\infty}^{\infty} \Psi(\mathbf{r}, t) \exp(-i\omega t) dt$$

$$S(\mathbf{r}, \omega) = \int_{-\infty}^{\infty} s(\mathbf{r}, t) \exp(-i\omega t) dt$$

and we have used the Fourier based definition for a fractional derivative, i.e.

$$\partial_t^q \Psi(\mathbf{r}, t) \leftrightarrow (-i\omega)^q \psi(\mathbf{r}, \omega)$$

so that

$$i^q \partial_t^q \Psi(\mathbf{r}, t) \leftrightarrow \omega^q \psi(\mathbf{r}, \omega)$$

where $\leftrightarrow$ denotes transformation from t-space to ω-space. The symbols $\otimes_\omega$ and $\odot_\omega$ denote the convolution and correlation integrals (in ω-space) respectively, i.e. for any complex piecewise continuous functions $f_1(\omega)$ and $f_2(\omega)$,

$$(f_1 \otimes_\omega f_2)(\omega) = \int_{-\infty}^{\infty} f_1(\omega - \omega') f_2(\omega') d\omega'$$

and

$$(f_1 \odot_\omega f_2^*)(\omega) = \int_{-\infty}^{\infty} f_1(\omega + \omega') f_2^*(\omega') d\omega'$$

4.1 Solution for $\mathbf{r} \in \mathbb{R}^3$ and $\omega \to 0$

In the infinite domain, the Green's function transformation, for $\mathbf{r} \in \mathbb{R}^3$, yield [35]

$$\psi(\mathbf{r}, \omega) = g(r, \omega) \otimes_{\mathbf{r}} S(\mathbf{r}, \omega)$$

$$+ g(r, \omega) \otimes_{\mathbf{r}} \kappa(2\pi)^2 [\psi(\mathbf{r}, \omega) \odot_\omega \psi^*(\mathbf{r}, \omega)] \otimes_\omega \psi(\mathbf{r}, \omega) \quad (6)$$

where $\otimes_{\mathbf{r}}$ denotes the convolution over $\mathbf{r}$ and g is the Green's function given by

$$g(\mathbf{r},\omega)=\frac{\exp(i\omega^{q/2})r}{4\pi r},\quad r\equiv\mid\mathbf{r}\mid$$

We now consider a solution based on a low frequency condition where

$$g(r,\omega)\sim\frac{1}{4\pi r},\quad \omega\in[-\Omega,\Omega],\quad \Omega\to 0$$

and a separation of variables approach where

$$\psi(\mathbf{r},\omega)=\phi(\mathbf{r})U(\omega)$$

and

$$S(\mathbf{r},\omega)=R(\mathbf{r})F(\omega)$$

The purpose of this is twofold:

(i) to consider low frequency wave propagation which is applicable to large scale ocean waves;

(ii) to investigate the temporal and spatial properties of (6) independently.

Equation (6) now becomes

$$\phi(\mathbf{r})U(\omega)=\frac{1}{4\pi r}\otimes_{\mathbf{r}}R(\mathbf{r})H(\omega)F(\omega)+$$

$$\frac{1}{4\pi r}\otimes_{\mathbf{r}}\kappa(2\pi)^2\mid\phi(\mathbf{r})\mid^2\phi(\mathbf{r})H(\omega)[U(\omega)\odot_{\omega}U^*(\omega)]\otimes_{\omega}U(\omega)$$

where

$$H(\omega)=\begin{cases}1, & \mid\omega\mid\leq\Omega;\\ 0, & \mid\omega\mid>\Omega.\end{cases}$$

so that, after inverse Fourier transforming, we obtain

$$\phi(\mathbf{r})u(t)=\frac{1}{4\pi r}\otimes_{\mathbf{r}}R(\mathbf{r})\frac{\Omega}{\pi}\mathrm{sinc}(\Omega t)\otimes_t f(t)$$

$$+\frac{1}{4\pi r}\otimes_{\mathbf{r}}\kappa\mid\phi(\mathbf{r})\mid^2\phi(\mathbf{r})\frac{\Omega}{\pi}\mathrm{sinc}(\Omega t)\otimes_t\mid u(t)\mid^2 u(t)$$

where

$$f(t)=\frac{1}{2\pi}\int_{-\infty}^{\infty}F(\omega)\exp(i\omega t)d\omega,$$

$$\frac{\Omega}{\pi}\mathrm{sinc}(\Omega t)\equiv\frac{\Omega}{\pi}\frac{\sin(\Omega t)}{\Omega t}=\frac{1}{2\pi}\int_{-\infty}^{\infty}H(\omega)\exp(i\omega t)d\omega$$

and $\otimes_t$ denotes the convolution integral over t. If we then apply the Laplacian operator, then, noting that

$$\nabla^2\left(\frac{1}{4\pi r}\right)=-\delta^3(\mathbf{r})$$

we have

$$u(t)\nabla^2\phi(\mathbf{r})=-\frac{\Omega}{\pi}\mathrm{sinc}(\Omega t)\otimes_t f(t)R(\mathbf{r})$$

$$-\kappa\frac{\Omega}{\pi}\mathrm{sinc}(\Omega t)\otimes_t\mid u(t)\mid^2 u(t)\mid\phi(\mathbf{r})\mid^2\phi(\mathbf{r})\qquad(7)$$

Thus, for any point in space $\mathbf{r}=\mathbf{r}_0$

$$u(t)=a\frac{\Omega}{\pi}\mathrm{sinc}(\Omega t)\otimes_t f(t)$$

$$+b\kappa\frac{\Omega}{\pi}\mathrm{sinc}(\Omega t)\otimes_t\mid u(t)\mid^2 u(t)$$

where

$$a=-\left[\frac{R(\mathbf{r})}{\nabla^2\phi(\mathbf{r})}\right]_{\mathbf{r}=\mathbf{r}_0}\quad\text{and}\quad b=-\left[\frac{\mid\phi(\mathbf{r})\mid^2\phi(\mathbf{r})}{\nabla^2\phi(\mathbf{r})}\right]_{\mathbf{r}=\mathbf{r}_0}$$

under the condition that $\mid\nabla^2\phi(\mathbf{r})\mid>0$ and

$$u(t)=0\quad\text{if}\quad\mid\nabla^2\phi(\mathbf{r})\mid_{\mathbf{r}=\mathbf{r}_0}=0$$

Similarly, at any point in time $t=t_0$

$$\nabla^2\phi(\mathbf{r})=\alpha R(\mathbf{r})+\beta\kappa\mid\phi(\mathbf{r})\mid^2\phi(\mathbf{r})$$

where, for $\mid u(t)\mid_{t=t_0}>0$,

$$\alpha=-\left[\frac{\Omega}{\pi u(t)}\mathrm{sinc}(\Omega t)\otimes_t f(t)\right]_{t=t_0},$$

$$\beta=-\left[\frac{\Omega}{\pi u(t)}\mathrm{sinc}(\Omega t)\otimes_t\mid u(t)\mid^2 u(t)\right]_{t=t_0}$$

and

$$\nabla^2\phi(\mathbf{r})=0\quad\text{if}\quad u(t)\mid_{t=t_0}=0$$

4.2 Solution for $\mathbf{r}\in\mathbb{R}^2$ and $\omega\to 0$

The same approach presented in the previous section can be used to obtain a solution for $\mathbf{r}\in\mathbb{R}^2$. However, there is an essential difference for $\mathbf{r}\in\mathbb{R}^2$ which derives from of the function form of the Green's function

$$g(r,\omega)=i\pi H_0^1(r\omega^{q/2})$$

where $H_0^{(1)}$ is Hankel function of first kind with the following asymptotic characteristics:

$$g(r,\omega)=\begin{cases}-2\ln(r\omega^{q/2}), & \omega\to 0;\\ \sqrt{\frac{2\pi}{r\omega^{q/2}}}\exp[i(r\omega^{q/2}+\pi/4)], & \omega\to\infty.\end{cases}$$

Thus under the low frequency bandwidth condition

$$g(r,\omega)=-2\ln r-q\ln\omega,\quad\omega\in[-\Omega,\Omega],\quad\Omega\to 0$$

Noting that

$$\nabla^2 \ln(r) = -\delta^2(\mathbf{r})$$

where

$$\nabla^2 \equiv \partial_x^2 + \partial_y^2,$$

in two-dimensions, (7) becomes

$$u(t)\nabla^2\phi(\mathbf{r}) = -2\frac{\Omega}{\pi}\text{sinc}(\Omega t) \otimes_t R(\mathbf{r})f(t)$$

$$-2\kappa\frac{\Omega}{\pi}\text{sinc}(\Omega t)\otimes_t \mid u(t) \mid^2 u(t) \mid \phi(\mathbf{r}) \mid^2 \phi(\mathbf{r})$$

Thus, apart from a scaling factor, the governing equations in $\mathbf{r} \in \mathbb{R}^2$ and $\mathbf{r} \in \mathbb{R}^3$ are identical. However, in this paper we focus of a two-dimensional model which is valid for surface waves.

4.3 Solution for $\mathbf{r} \in \mathbb{R}^1$ and $\omega \to 0$

Although a one-dimensional model is of little value to modelling sea surface waves, for completeness, we present the equivalent solution for $\mathbf{r} \in \mathbb{R}^1$. In this case, the Green's function is given by

$$g(\mid x \mid, \omega) = \frac{i}{2\omega^{q/2}} \exp(i\omega^{q/2} \mid x \mid)$$

$$= \frac{i}{2\omega^{q/2}}[1 + i\omega^{q/2} \mid x \mid + \frac{1}{2}(i\omega^{q/2} \mid x \mid)^2 + ...]$$

and thus, for $\mid \omega \mid \leq \Omega$ where Ω is the bandwidth of the wave function, we can approximate the Green's function as

$$g(\mid x \mid, \omega) = \frac{i}{2\omega^{q/2}} - \frac{\mid x \mid}{2}, \quad \mid \omega \mid \leq \Omega \to 0$$

Thus for $\mathbf{r} \in \mathbb{R}^1$, we have

$$\phi(x)U(\omega) = \frac{iR_1H(\omega)}{2\omega^{q/2}}F(\omega) - R_2(x)H(\omega)F(\omega)$$

$$+\frac{i\kappa(2\pi)^2\Phi_1H(\omega)}{2\omega^{q/2}}\{[U(\omega) \odot_\omega U^*(\omega)] \otimes_\omega U(\omega)\}$$

$$-\kappa(2\pi)^2\Phi_2(x)H(\omega)\{[U(\omega) \odot_\omega U^*(\omega)] \otimes_\omega U(\omega)\}$$

where

$$R_1 = \int_{-\infty}^{\infty} R(x)dx,$$

$$R_2(x) = \frac{\mid x \mid}{2} \otimes_x R(x),$$

$$\Phi_1 = \int_{-\infty}^{\infty} \mid \phi(x) \mid^2 \phi(x)dx$$

and

$$\Phi_2(x) = \frac{\mid x \mid}{2}\otimes_x \mid \phi(x) \mid^2 \phi(x)$$

Hence, since $\mid x \mid = x\text{sign}(x)$ where $\text{sign}(x)$ is the 'sign' function defined as

$$\text{sign}(x) = \begin{cases} 1, & x > 0; \\ -1, & x < 0. \end{cases}$$

and noting that $\text{sign}(x) = 2\text{step}(x) - 1$ where

$$\text{step}(x) = \begin{cases} 1, & x > 0; \\ 0, & x < 0. \end{cases}$$

then

$$\frac{d}{dx}R_2(x) = \frac{1}{2}\text{sign}(x) \otimes_x R(x)$$

$$= \text{step}(x) \otimes_x R(x) - \frac{1}{2}R_1$$

and

$$\frac{d^2}{dx^2}R_2(x) = R(x) \quad \text{since} \quad \frac{d}{dx}\text{step}(x) = \delta(x)$$

Similarly

$$\frac{d^2}{dx^2}\Phi_2(x) = \mid \phi(x) \mid^2 \phi(x)$$

so that, after inverse Fourier transforming, we obtain

$$u(t)\frac{d^2}{dx^2}\phi(x) = -R(x)\frac{\Omega}{\pi}\text{sinc}(\Omega t) \otimes_t f(t)$$

$$-\frac{\kappa\Omega}{\pi}\text{sinc}(\Omega t) \mid u(t) \mid^2 u(t) \mid \phi(x) \mid^2 \phi(x)$$

4.4 Source Function Models

Any solution for $\Psi(\mathbf{r}, t) = \phi(\mathbf{r})u(t)$ depends explicitly on the source function $R(\mathbf{r})f(t)$. Physically, $f(t)$ represents the variations in the wave amplitude generated by changes in the wind velocity $v(t)$ thereby producing an acceleration/deceleration and thus a force that 'drives' the wave motion. On the other hand $R(\mathbf{r})$ is determined by the spatial frequency content of the sea surface. We now consider stochastic models for these function.

4.4.1 Stochastic Model for $R(\mathbf{r})$, $\mathbf{r} \in \mathbb{R}^2$

We require a model for the spatial frequency characteristics (i.e. the Power Spectral Density Function) of the stochastic field $R(\mathbf{r})$ representing the sea surface at an instance in time. To this end, we consider a PSDF of the form

$$P(k) = \frac{k^{2p}}{(k_0^2 + k^2)^q} = \left|\frac{(ik)^p}{(k - ik_0)^q}\right|^2$$

where $k = \mid \mathbf{k} \mid$ which is a generalization of the Berman processes where [36]

$$P(k) = \frac{k^{2p}}{k_0^2 + k^2}$$

that is, in turn, a generalization of the Ornstein-Uhlenbeck processes where [37], [38] and [39]

$$P(k) = \frac{k}{k_0^2 + k^2}$$

with parameters c and k_0, $p > 0$ and $q > 0$. The parameters p, q and k_0 provides a way of 'shaping' the PSDF of the stochastic field $R(\mathbf{r})$ as illustrated in Figure 2.

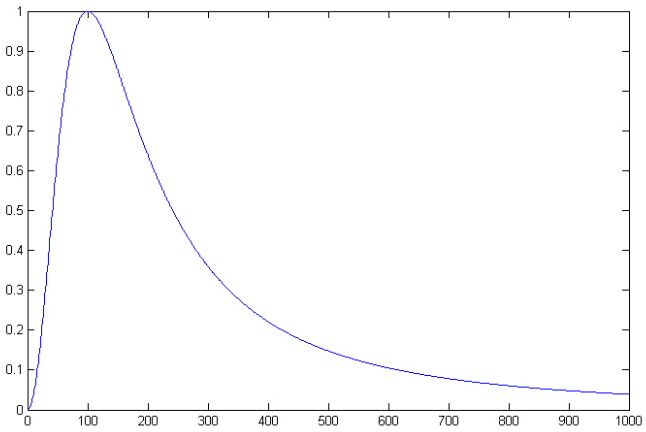

Figure 2: Normalised plot of the PSDF $k^{2p}(k_0^2 + k^2)^{-q}$ for $k_0 = 100$, $p = 1$, $q = 2$ and an array length of 1000 elements.

For $k > 0$, the function $P(k) > 0 \forall k$ has a maximum when

$$\frac{d}{dk} \ln P(k) = \frac{2p}{k} - \frac{2kq}{k_0^2 + k^2} = 0$$

or when

$$\frac{d}{dk} P(k) = \left(\frac{2p}{k} - \frac{2kq}{k_0^2 + k^2} \right) P(k) = 0$$

This implies that the maximum value of $P(k)$ occurs at a value of $k = k_{\max}$ given by

$$k_{\max} = k_0 \sqrt{\frac{p}{q-p}}, \quad q > p$$

The value of $P(k)$ at this point is therefore

$$P_{\max} \equiv P(k_{\max}) = \frac{k_{\max}^{2p}}{(k_0^2 + k_{\max}^2)^q} = k_0^{2(p-q)} \frac{p^p}{q^q} (q-p)^{q-p}$$

Beyond this point, the PSDF decays and its asymptotic form is dominated by a k^{-2q} power law, a law that is consistent with a random scaling fractal. At low frequencies, the power spectrum is characterized by the term k^{2p}. The parameter k_0 defines the principal spatial frequency (as illustrated in Figure 2) of the stochastic function $R(\mathbf{r})$, that, using the Riesz operator, is given by

$$R(\mathbf{r}) = \frac{1}{(2\pi)^2} \int_{-\infty}^{\infty} \left[\frac{(ik)^p}{(k - ik_0)^q} N(\mathbf{k}) \right] \exp(i\mathbf{k} \cdot \mathbf{r}) d^2\mathbf{k}$$

$$= K(\mathbf{r}) \otimes_{\mathbf{r}} \nabla^p n(\mathbf{r})$$

where $N(\mathbf{k})$ is a white noise spectrum (with constant PSDF),

$$n(\mathbf{r}) = \frac{1}{(2\pi)^2} \int_{-\infty}^{\infty} N(\mathbf{k}) \exp(i\mathbf{k} \cdot \mathbf{r}) d^2\mathbf{k}$$

and

$$K(\mathbf{r}) = \frac{1}{(2\pi)^2} \int_{-\infty}^{\infty} \left[\frac{1}{(k - ik_0)^q} \right] \exp(i\mathbf{k} \cdot \mathbf{r}) d^2\mathbf{k}$$

Since (as derived in Appendix A)

$$\int_{-\infty}^{\infty} r^{q-2} \exp(-ik\hat{\mathbf{n}} \cdot \mathbf{r}) d^2\mathbf{r} = \frac{1}{(2i)^q \pi} \frac{\Gamma\left(1 - \frac{q}{2}\right)}{\Gamma\left(\frac{q}{2}\right)} \frac{1}{k^q}$$

then

$$\int_{-\infty}^{\infty} r^{q-2} \exp[-i(k - ik_0)\hat{\mathbf{n}} \cdot \mathbf{r}] d^2\mathbf{r}$$

$$= \frac{1}{(2i)^q \pi} \frac{\Gamma\left(1 - \frac{q}{2}\right)}{\Gamma\left(\frac{q}{2}\right)} \frac{1}{(k - ik_0)^q}$$

and thus

$$K(\mathbf{r}) = \frac{(2i)^q \pi \Gamma\left(\frac{q}{2}\right)}{\Gamma\left(1 - \frac{q}{2}\right)} \exp(-k_0 \hat{\mathbf{n}} \cdot \mathbf{r}) r^{q-2}$$

Hence, ignoring scaling,

$$R(\mathbf{r}) = \frac{\exp(-k_0 \hat{\mathbf{n}} \cdot \mathbf{r})}{r^{2-q}} \otimes_{\mathbf{r}} \nabla^p n(\mathbf{r})$$

whose random scaling property is

$$\Pr[R(a\mathbf{r}, k_0/a)] = a^{q-p} \Pr[R(\mathbf{r}, k_0)]$$

Here, as we scale $\mathbf{r}$ by a, the characteristic frequency k_0 is scaled by $1/a$, a result that relates to the scaling property of the Fourier transform, i.e.

$$R(a\mathbf{r}) \leftrightarrow \frac{1}{a} R\left(\frac{\mathbf{k}}{a}\right)$$

The interpretation of this result is that, as we zoom into the stochastic field $R(\mathbf{r}, k_0)$, the distribution of amplitudes remains the same (subject to scaling by a^{p-q}) and the characteristic frequency of the field increases by a factor of $1/a$. Finally, we apply a spatial frequency 'bias' by letting

$$k = \sqrt{[(L_x k_x)^2 + (L_y k_y)^2]}$$

in order to give a directionality to the surface waves generated by a prevailing wind direction. Thus if $L_x = L_y = 1$, the wind is taken to be omni- directional whereas if $L_x = 0$ and $L_y = 1$, for example, then the effect is to lowpass the spectrum of $N(k_x, k_y)$ in k_y alone, thereby generating a stochastic field $R(x, y)$ with a high frequency x-directional bias.

4.4.2 Stochastic Model for $f(t)$

If $f(t)$ represents the force of the wind on the sea surface at any time t then the function

$$g(t) = \frac{\Omega}{\pi}\text{sinc}(\Omega t) \otimes_t f(t)$$

given in (7), models the conversion of this force into that which 'drives' the wave motion of the sea surface. The bandwidth Ω limits the frequency spectrum at which this conversion takes place due to the change in density at the boundary between the air and the sea surface. For a unit mass, $f(t)$ is given by (from Newton's second law of motion)

$$f(t) = d_t v(t)$$

Thus, in order to compute a suitable stochastic model for $f(t)$, it is necessary to analyse the stochastic behaviour of the wind velocity $v(t)$ and in the following section this is explored using experimental data.

5 Statistical Analysis of the Wind Velocity

The statistical analysis of wind velocity provides a route to developing stochastic models for wind speed including those used in forecasting [40]. In this section we consider a stochastic model for the wind velocity that is designed to provide a stochastic source function for the generation of sea surface waves. In particular, we are interested in the time variations associated with the source function $s(\mathbf{r}, t)$ given in equation (5).

Figure 3 shows a polar plot of experimental data for hourly wind velocities (in metres per second) against wind directions (in degrees). The data consists of 8000 samples recorded at Dublin Airport, Ireland from 00:00:00 on 1 January 2008 to 06:00:00 on 29 November 2008. The maximum wind velocity is 21.1ms^{-1}.

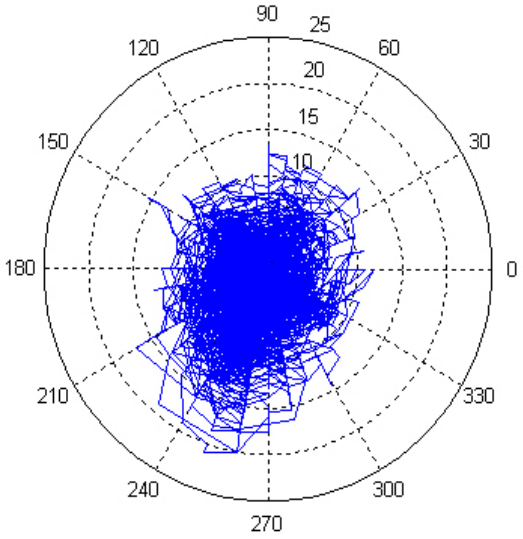

Figure 3: Polar plot of the angle of wind direction versus the wind velocity (in metres per second) over a period of 8000 hours for 1 hour sampling intervals.

Figure 4 show plots of the wind velocity and wind direction together with associated histograms illustrating a marked difference in their statistical characteristics. The wind velocity has a Rayleigh-type distribution with a mode of 5ms^{-1} whereas the wind direction is has a marked statistical bias toward higher angles with a primary mode of 240 degrees accounting for the directional bias observed in Figure 3.

Figure 5 compares the velocity gradient $f(t)$ (which represents the force generated by the wind for a unit mass computed by forward differencing) with the output from a Gaussian distributed random number stream (with zero-mean). By comparing these number streams, it is clear that the statistical characteristics of $f(t)$ are not Gaussian. The plot of $f(t)$ obtained from the experimental wind velocity data clearly shows that there are a number of rare but extreme events corresponding to short periods of time over which the change in wind velocity is relatively high. This leads to a distribution with a narrow width but longer tail (when compared to a normal distribution). Non-Gaussian distributions of this type are typical of Lévy processes [29], [30] which are discussed in the following section.

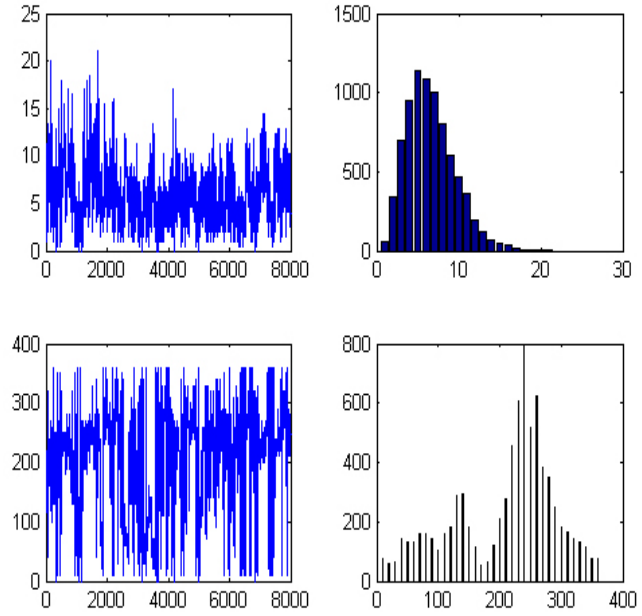

Figure 4: Plots of the wind velocity (top-left in metres per second) and wind direction (bottom-left in degrees) and the associated 21-bin and 360-bin histograms (top-right and bottom-right), respectively.

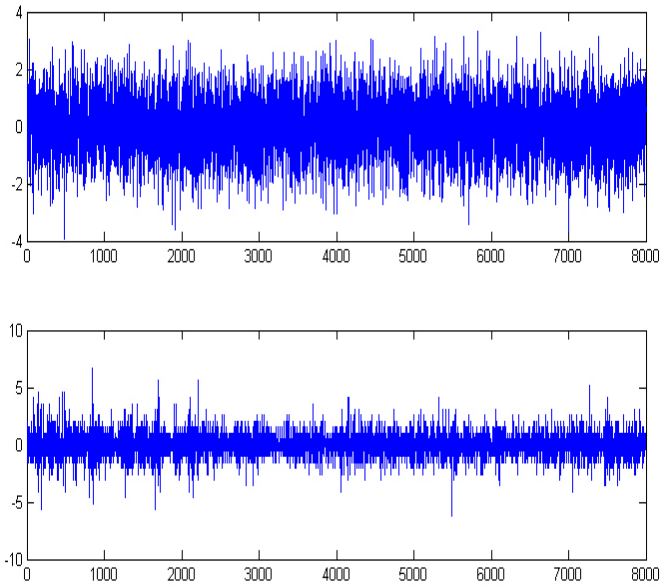

Figure 5: Plots of a zero-mean Gaussian distributed stochastic signal (bottom-left) obtained using MATLAB V7 *randn* function (above) and gradient of the wind velocity given in Figure 5 (below).

5.1 Lévy Processes

Lévy processes are random walks whose distribution has infinite moments. The statistics of (conventional) physical systems are usually concerned with stochastic fields that have PDFs where (at least) the first two moments (the mean and variance) are well defined and finite. Lévy statistics is concerned with statistical systems where all the moments (starting with the mean) are infinite. Many distributions exist where the mean and variance are finite but are not representative of the process, e.g. the tail of the distribution is significant, where rare but extreme events occur. These distributions include Lévy distributions [31], [32] and [33]. Lévy's original approach to deriving such distributions is based on the following question: Under what circumstances does the distribution associated with a random walk of a few steps look the same as the distribution after many steps (except for scaling)? This question is effectively the same as asking under what circumstances do we obtain a random walk that is statistically self-affine. The characteristic function $P(k)$ of such a distribution $p(x)$ was first shown by Lévy to be given by (for symmetric distributions only)

$$P(k) = \exp(-a \mid k \mid^{\gamma}), \quad 0 < \gamma \leq 2 \tag{8}$$

where a is a constant and γ is the Lévy index. For $\gamma \geq 2$, the second moment of the Lévy distribution exists and the sums of large numbers of independent trials are Gaussian distributed. For example, if the result were a random walk with a step length distribution governed by $p(x)$, $\gamma \geq 2$, then the result would be normal (Gaussian) diffusion, i.e. a Brownian random walk process. For $\gamma < 2$ the second moment of this PDF (the mean square), diverges and the characteristic scale of the walk is lost. For values of γ between 0 and 2, Lévy's characteristic function corresponds to a PDF of the form

$$p(x) \sim \frac{1}{x^{1+\gamma}}, \quad x \to \infty$$

Lévy processes are consistent with a fractional diffusion equation as we shall now show [34]. The evolution equation for a random walk process leading to a macroscopic field denoted by $v(x,t)$ is given by

$$v(x, t+\tau) = v(x,t) \otimes_x p(x)$$

which, in Fourier space, is

$$V(k, t+\tau) = V(k,t)P(k)$$

From (8), we note that

$$P(k) = 1 - a \mid k \mid^{\gamma}, \quad a \to 0$$

so that we can write

$$\frac{V(k,t+\tau)-V(k,t)}{\tau} \simeq -\frac{a}{\tau} \mid k \mid^{\gamma} V(k,t)$$

which for $\tau \to 0$ gives the fractional diffusion equation

$$\sigma \frac{\partial}{\partial t} v(x,t) = \frac{\partial^{\gamma}}{\partial x^{\gamma}} v(x,t), \quad \gamma \in (0,2] \tag{9}$$

where $\sigma = \tau/a$ and we have used the result

$$\frac{\partial^{\gamma}}{\partial x^{\gamma}} v(x,t) = -\frac{1}{2\pi} \int_{-\infty}^{\infty} \mid k \mid^{\gamma} V(k,t) \exp(ikx) dk$$

The solution to this equation with the singular initial condition $v(x,0) = \delta(x)$ is given by

$$v(x,t) = \frac{1}{2\pi} \int_{-\infty}^{\infty} \exp(ikx - t \mid k \mid^{\gamma} / \sigma) dk$$

which is itself Lévy distributed. This derivation of the fractional diffusion equation reveals its physical origin in terms of Lévy statistics.

For normalized units $\sigma = 1$ we consider (9) for a white noise source $n(t) \in [0,1] \forall t$ with $\Pr[n(t)] = 1$ given by

$$\frac{\partial^{\gamma}}{\partial x^{\gamma}} v(x,t) - \frac{\partial}{\partial t} v(x,t) = -\delta(x) n(t), \quad \gamma \in (0,2]$$

which, at $x = 0$ has the Green's function solution

$$v_0(t) = \frac{1}{\Gamma(1/\gamma) t^{1-1/\gamma}} \otimes_t n(t) \tag{10}$$

where $v_0(t) \equiv v(0,t)$. This equation is an example of fractional stochastic partial differential equations used to model Lévy noise compared to a stochastic partial differential equations with Lévy noise [41].

The function v_0 has a Power Spectral Density Function (PSDF) given by (for constant of proportionality c)

$$\mid V_0(\omega) \mid^2 = \frac{c}{\mid \omega \mid^{2/\gamma}}$$

where

$$V_0(\omega) = \int_{-\infty}^{\infty} v_0(t) \exp(-i\omega t) dt$$

and a self-affine scaling relationship

$$\Pr[v_0(at)] = a^{1/\gamma} \Pr[v_0(t)]$$

for scaling parameter $a > 0$. This scaling relationship means that the statistical characteristics of $v_0(t)$ is invariant of the time scale.

5.2 Lévy Index Analysis

The PSDF of $\mid V_0(\omega) \mid^2$ provides a method of computing γ using the least squares method based on minimizing the error function

$$e(c,\gamma) = \| 2 \ln \mid V_0(\omega) \mid - \ln c - 2\gamma^{-1} \ln \mid \omega \mid \|_2^2, \quad \omega > 0$$

Figure 6 shows the computation of $\gamma(t)$ for a moving window of size 1024 elements. Table 2 provides some

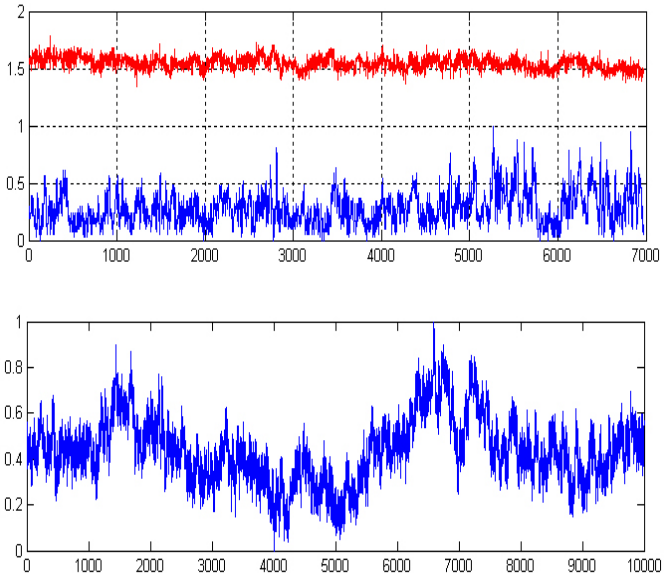

Figure 6: Above: Plot of the wind velocity given in Figure 4 after normalization (blue) and the Lévy index (red) obtained using a moving window is size 1024 elements. Below: Simulated wind velocities computed for Lévy index $\gamma = 1.55$

basic statistical information with regard to $\gamma(t)$ for this data. Application of the Bera-Jarque parametric hypothesis test of composite normality is rejected (i.e. 'Composite Normality' is of type 'Reject') and thus $\gamma(t)$ is not normally distributed. This result illustrates that the wind velocity function is a self-affine stochastic function with a mean Lévy index of 1.55. Based on this result, Figure 6 shows a simulation of the wind velocity based on the computation of $v_0(t)$ in (10) for $\gamma = 1.55$. The simulation is based on transforming (10) into Fourier space and using a Discrete Fourier Transform. The function $n(t)$ is computed using MATLAB (V7) uniform random number generator *rand* for *seed* = 1.

Table 2: Statistical parameters associated with the Lévy index function given in Figure 6.

Statistical Parameter	Value for $\gamma(t)$
Minimum Value	1.3467
Maximum value	1.7836
Range	0.4369
Mean	1.5490
Median	1.5493
Standard Deviation	0.0522
Variance	0.0027
Skewness	0.0106
Kertosis	2.7833
Composite Normality	Reject

6 Iterative Solutions

We consider iterative solutions to the equations

$$u(t) = \frac{\Omega}{\pi}\text{sinc}(\Omega t) \otimes_t f(t) + \kappa\frac{\Omega}{\pi}\text{sinc}(\Omega t) \otimes_t u(t) \mid u(t) \mid^2 \tag{11}$$

where $f(t) = d_t v_0(t)$ and

$$\nabla^2\phi(\mathbf{r}) = R(\mathbf{r}) + \kappa\phi(\mathbf{r}) \mid \phi(\mathbf{r}) \mid^2, \quad \mathbf{r} \in \mathbb{R}^2 \tag{12}$$

6.1 Temporal Solution

We consider an iterative solution to (11) of the form (for $n = 0, 1, 2, ..$)

$$u_{n+1}(t) = \frac{\Omega}{\pi}\text{sinc}(\Omega t) \otimes_t f(t)$$

$$+\kappa\frac{\Omega}{\pi}\text{sinc}(\Omega t) \otimes_t u_n(t) \mid u_n(t) \mid^2$$

The convergence criterion for this solution is derived in Appendix B where it is shown that

$$\|u(t)\|_2^2 < \frac{1}{3\kappa}\sqrt{\frac{\pi}{\Omega}}$$

We therefore consider the first order approximation for the signal $u_1(t)$ given by

$$u_1(t) = \bar{f}(t) + \kappa\frac{\Omega}{\pi}\text{sinc}(\Omega t) \otimes_t \bar{f}(t) \mid \bar{f}(t) \mid^2 \tag{13}$$

where

$$\bar{f}(t) = \frac{\Omega}{\pi}\text{sinc}(\Omega t) \otimes_t f(t)$$

under the condition

$$\|u(t)\|_2^2 << \frac{1}{3\kappa}\sqrt{\frac{\pi}{\Omega}}$$

This solution is equivalent to application of the Born approximation for Schrödinger scattering theory when the (time-independent) potential $V(\mathbf{r}), \quad \mathbf{r} \in \mathbb{R}^3$ is taken to be a 'weak scatterer' subject to the condition $\|V\|_2 << R^{-2}, \quad r \in [0, R]$.

We require a numerical simulation for $u_1(t)$ to investigate the effect of the nonlinear term in (13) given that

$$f(t) = \frac{1}{\Gamma(1/\gamma)t^{1-1/\gamma}} \otimes_t d_t n(t) \tag{14}$$

where $n(t) \in [0, 1]$ and $\Pr[n(t)] = 1$ and the normalisation condition $\|\bar{f}(t)\|_\infty = 1$. The numerical simulation is obtained by transforming (13) and (14) into Fourier space and using a Discrete Fourier Transform to filter the array $n[i]$ and inverse Fourier transforming the result. Figure 7 shows an example of the computation of $u_1[i], \quad i = 1, 2, ..., N$ for $N = 1000$ and with $\Omega = 15$ and $\gamma = 1.55$ using MATLAB (V7) function *rand* with *seed* $= 1$ to compute $n[i]$. For $q = 1$, Figure 7 illustrates the influence of the nonlinear term in (13) with regard to generating waves whose amplitudes are in excess of the corresponding linear waves. The relatively high amplitude wave obtained between line elements 400 and 500 in Figure 7, which are typical of simulation based on (13), exhibits an abyssal trough commonly seen before and after a freak wave that in practice may last only for some minutes before either breaking, or reducing in size. With regard the model used, it is clear that this behaviour depends on the magnitude of the source function $f(t)$ and that this function is determined by the characteristics of $v_0(t)$ as determined by the Lévy index γ. For large changes in $v_0(t)$ where the force of the wind $f(t) = d_t v_0(t)$ is high, the likelihood of a freak wave is increased. This likelihood is a result of the non-Gaussian distribution assumed for $f(t)$, as illustrated in Figure 5, where, compared to Gaussian distributed deviates, rare but extreme values can occur.

6.2 Spatial Solution

The Green's function transformation to (12) is (for the infinite domain) given by

$$\phi(\mathbf{r}) = -\ln(r) \otimes_2 [R(\mathbf{r}) + \kappa \mid \phi(\mathbf{r}) \mid^2 \phi(\mathbf{r})] \tag{15}$$

which has the iterative solution (for $n = 0, 1, 2, ...$)

$$\phi_{n+1}(\mathbf{r}) = -\ln(r) \otimes_2 [R(\mathbf{r}) + \kappa \mid \phi_n(\mathbf{r}) \mid^2 \phi_n(\mathbf{r})]$$

where

$$\phi_0(\mathbf{r}) = -\ln(r) \otimes_2 R(\mathbf{r})$$

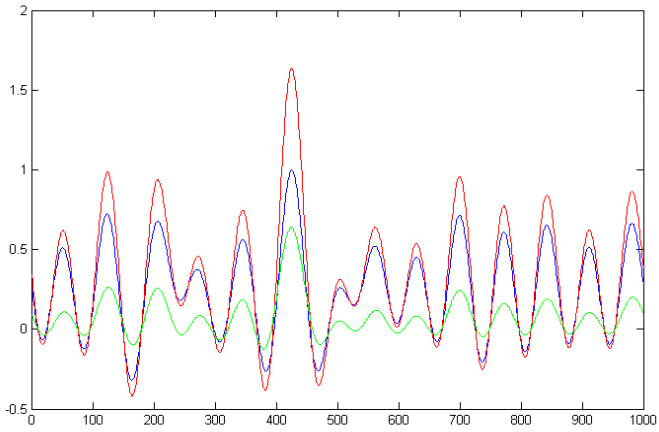

Figure 7: Simulation of $u_1[i]$ for $q = 2$ (Blue) and for $q = 1$ (Red). The nonlinear term given in (13) is shown in Green.

with convergence criterion (derived in Appendix C) given by

$$\|\Phi(\mathbf{r})\| < \left(\frac{2}{9\pi\kappa^2}\right)^{\frac{1}{4}}, \quad r \in [0,1]$$

and where, based on the model discussed in Section 4.4.1,

$$R(\mathbf{r}) = \frac{\exp(-k_0\hat{\mathbf{n}}\cdot\mathbf{r})}{r^{2-q}} \otimes_{\mathbf{r}} \nabla^p n(\mathbf{r})$$

We consider an approximate first order solution ϕ_1 for ϕ given by

$$\phi_1(\mathbf{r}) = \ln(r) \otimes_2 R(\mathbf{r}) + \kappa \mid \ln(r) \otimes_2 R(\mathbf{r}) \mid^2 [\ln(r) \otimes_2 R(\mathbf{r})] \tag{16}$$

based on the computation of $\ln(r) \otimes_{\mathbf{r}} R(\mathbf{r})$ in Fourier space using a Fast Fourier Transform, i.e.

$$\ln(r) \otimes_{\mathbf{r}} R(\mathbf{r}) \leftrightarrow \frac{1}{k^2} \frac{(ik)^p}{(k - ik_0)^q} N(\mathbf{k}), \quad k > 0$$

For the linear case in which $q = 2$, Figure 8 illustrates the effect of increasing the spatial frequency via the parameter p for $L_x = 0$, $L_y = 1$ and $k_0 = 50$ based on using a zero mean random Gaussian field $n(x, y)$.

Figure 9 shows an example of ϕ_1 given by (16) for $(k_0, L_x, L_y, p, q) = (50, 0, 1, 0.99, 2)$ and $(k_0, L_x, L_y, p, q) = (50, 0, 1, 0.99, 1)$ based on using a zero mean random Gaussian field $n(x, y)$. The normalized surface plots illustrate the influence of the nonlinear term to produce a single 'freak wave' for $q = 1$.

7 Scattering Model for a Freak Wave

One of the principal issues associated with using the (cubic) NLS equation to model freak waves is that it is based

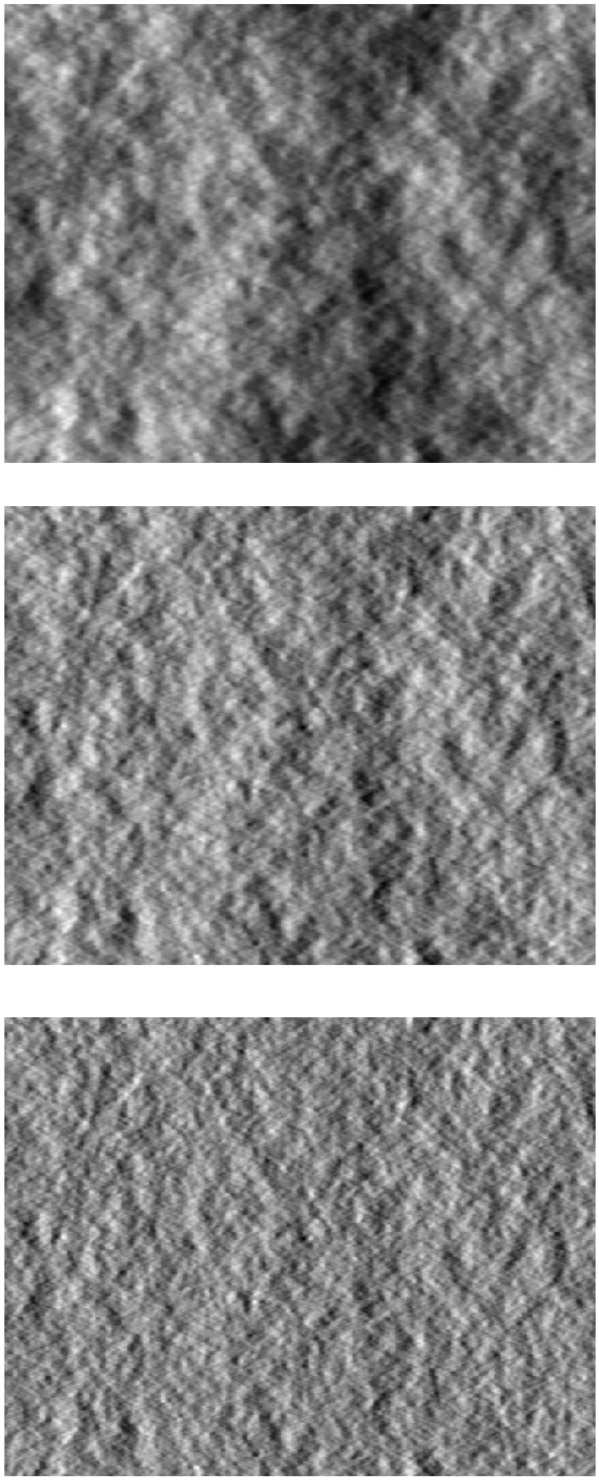

Figure 8: Examples of the stochastic surfaces ϕ_1 obtained using (16) - visualized as 512×512, 8-bit grey level images - for $(k_0, L_x, L_y, q) = (50, 0, 1, 2)$ with $p = 1.1$ (top), $p = 1.5$ (centre) and $p = 1.9$ (bottom) computed using the MATLAB (V7) random number generating function *randn* for *seed* = 1.

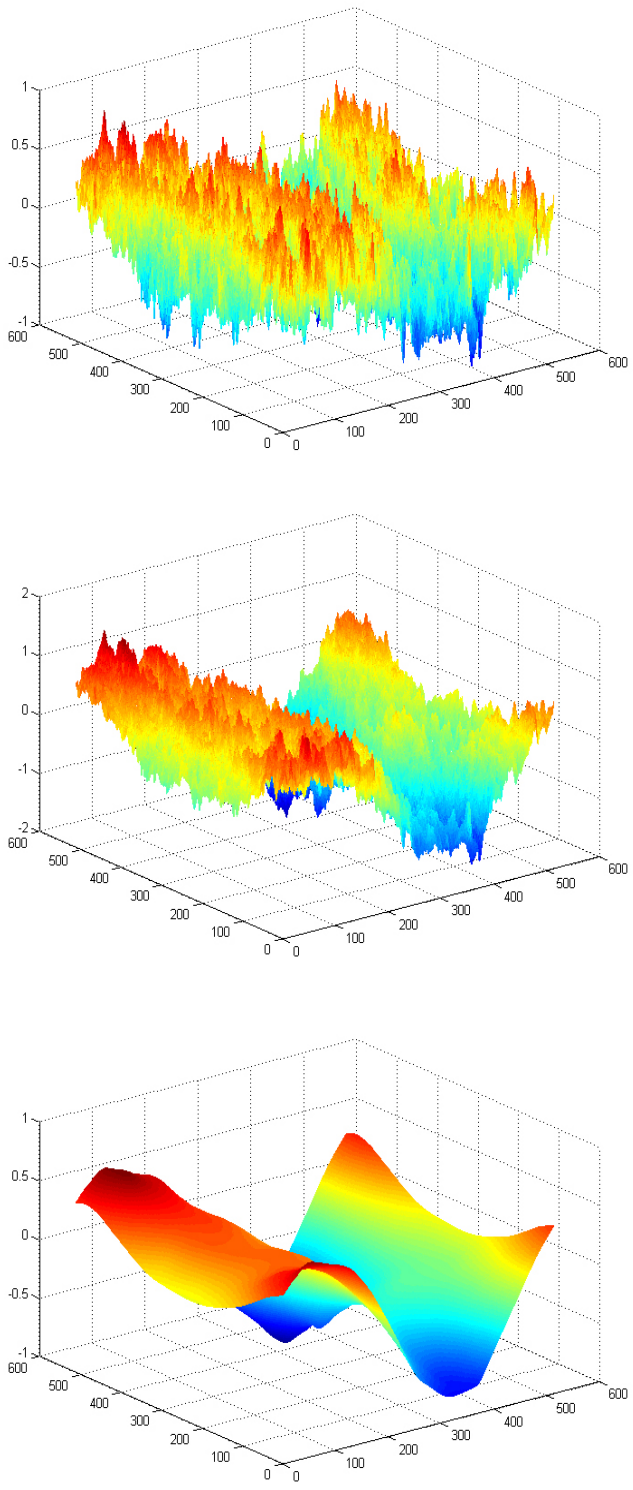

Figure 9: Comparison of a low frequency linear wave function $\phi_1(x,y)$, $q=2$ (above), a low frequency nonlinear wave function $\phi_1(x,y))$, $q=1$ (centre) based on (16). The associated nonlinear function is given below computed using the MATLAB (V7) random number generating function *randn* with *seed* = 1.

on a phenomenology, like the Schrödinger equation itself (linear of otherwise). In this section, we illustrate how to obtain analogous (nonlinear) behaviour based on a novel approach to solving the Helmholtz scattering problem which, in turn, is based on the classical wave equation for variable wavespeed. We consider a solution to this equation based on a phase only condition for the sum of the incident and scattered wavefield and aim to develop a solution that provides a model for the time evolution of a freak wave.

7.1 Inhomogeneous Wave Equation

Consider the inhomogeneous wave equation for $\mathbf{r} \in \mathbb{R}^3$ for a source function $s(\mathbf{r},t)$ given by

$$\left(\nabla^2 - \frac{1}{c^2(\mathbf{r})}\frac{\partial^2}{\partial t^2}\right)\Psi(\mathbf{r},t) = -s(\mathbf{r},t)$$

where $c(\mathbf{r})$ is the wavespeed function and let

$$\Psi(\mathbf{r},t) = \frac{1}{(2\pi)^3}\int_{-\infty}^{\infty}\psi(\mathbf{r},\omega)\exp(i\omega t)d\omega$$

and

$$s(\mathbf{r},t) = \frac{1}{(2\pi)^3}\int_{-\infty}^{\infty}S(\mathbf{r},\omega)\exp(i\omega t)d\omega$$

so that, with

$$\frac{1}{c^2(\mathbf{r})} = \frac{1}{c_0^2}[1+\gamma(\mathbf{r})]$$

we can write

$$\left(\nabla^2 + k^2\right)\psi(\mathbf{r},\omega) = -k^2\gamma(\mathbf{r})\psi(\mathbf{r},\omega) - S(\mathbf{r},\omega)$$

where $k = \omega/c_0$ and γ is the 'scattering function'. Appendix D provides a derivation of this result using the (linearised) Navier-Stokes equations where it is shown that Ψ represents the scalar velocity field and γ represents variations in the material density for the case when the viscosity is negligible and the compressibility is a constant. In particular, the scattering function is given by

$$\gamma_\rho(\mathbf{r}) = \frac{\rho(\mathbf{r}) - \rho_0}{\rho_0}$$

where ρ_0 is the 'average density'.

Let

$$\psi(\mathbf{r},\omega) = \psi_i(\mathbf{r},\omega) + \psi_s(\mathbf{r},\omega)$$

where ψ_s is the scattered field whose solution we require and ψ_i is the solution of

$$(\nabla^2 + k^2)\psi_i(\mathbf{r},\omega) = -S(\mathbf{r},\omega)$$

given by

$$\psi_i(\mathbf{r},\omega) = \frac{\exp(ikr)}{4\pi r} \otimes_{\mathbf{r}} S(\mathbf{r},\omega)$$

The equation

$$\left(\nabla^2 + k^2\right)(\psi_i + \psi_s) = -k^2\gamma_\rho(\psi_i + \psi_s) - S$$

is then reduced to

$$\left(\nabla^2 + k^2\right)\psi_s = -k^2\gamma_\rho\psi \tag{17}$$

However, since

$$\nabla^2\left(\frac{1}{4\pi r}\right) = -\delta^3$$

we can write

$$\left(\nabla^2 + k^2\right)\psi_s = \nabla^2\left[\left(\delta^3 - \frac{k^2}{4\pi r}\right) \otimes_{\mathbf{r}} \psi_s\right]$$

$$= \left(\delta^3 - \frac{k^2}{4\pi r}\right) \otimes_{\mathbf{r}} \nabla^2\psi_s$$

and thus

$$\frac{1}{4\pi r_+} \otimes_{\mathbf{r}} \nabla^2\psi_s = \gamma_\rho\psi$$

or

$$\psi_s(\mathbf{r}) = -\gamma_\rho(\mathbf{r})\psi(\mathbf{r},k)$$

where we have used the result

$$\frac{1}{4\pi r_+} \otimes_{\mathbf{r}} \nabla^2\psi_s = \psi_s \otimes_{\mathbf{r}} \nabla^2\left(\frac{1}{4\pi r_+}\right) \sim -\psi_s, \quad r_+ \to r$$

In the context of this result, we require a solution for the scattered field that satisfies the equation

$$\psi_i^*\psi_s + \mid \psi_s \mid^2 = -\gamma_\rho \mid \psi \mid^2$$

This result is consistent with the application of a low spatial frequency condition since in Fourier space equation (17) can be written as

$$(-u^2 + k^2)\widetilde{\psi}_s(\mathbf{u},\omega) = -k^2\widetilde{\gamma}_\rho(\mathbf{u}) \otimes_{\mathbf{u}} \widetilde{\psi}(\mathbf{u},\omega)$$

where $u \equiv \mid \mathbf{u} \mid$,

$$\widetilde{\psi}_s(\mathbf{u},\omega) = \int_{-\infty}^{\infty} \psi_s \exp(-i\mathbf{u}\cdot\mathbf{r}) d^3\mathbf{r},$$

$$\widetilde{\psi}(\mathbf{u},\omega) = \int_{-\infty}^{\infty} \psi \exp(-i\mathbf{u}\cdot\mathbf{r}) d^3\mathbf{r}$$

and

$$\widetilde{\gamma}_\rho(\mathbf{u}) = \int_{-\infty}^{\infty} \gamma_\rho(\mathbf{r}) \exp(-i\mathbf{u}\cdot\mathbf{r}) d^3\mathbf{r}$$

Thus, if

$$k^2 - u^2 = k^2\left(1 - \frac{u^2}{k^2}\right) \sim k^2, \quad u/k << 1$$

then

$$\widetilde{\psi}_s(\mathbf{u},\omega) = -\widetilde{\gamma}_\rho(\mathbf{u}) \otimes_{\mathbf{u}} \widetilde{\psi}(\mathbf{u},\omega)$$

or

$$\psi_s(\mathbf{r},\omega) = -\gamma_\rho(\mathbf{r})\psi(\mathbf{r},\omega)$$

where the functions γ_ρ, ψ and ψ_s are taken to be 'low-band-pass' functions, e.g. $\widetilde{\gamma}_\rho(\mathbf{u}) \to 0$ as $u \to \infty$. This implies that all functions in equation (17) are taken to be smooth in the sense that they are piecewise continuous and differentiable. Similarly, we note that, under the condition $u/k << 1$,

$$\psi_i(\mathbf{r},\omega) = -S(\mathbf{r},\omega)$$

7.2 Phase Only Solution

If we consider the function $\psi(\mathbf{r},\omega)$ to be a phase only wavefield where, for unit amplitude,

$$\psi(\mathbf{r},\omega) = \exp[i\theta_\psi(\mathbf{r},\omega)]$$

then

$$\psi_s = -\frac{\psi_i}{\mid \psi_i \mid^2}(\gamma_\rho + \mid \psi_s \mid^2)$$

which has first and second order solutions given by

$$\psi_s^{(1)} = -\frac{\gamma_\rho\psi_i}{\mid \psi_i \mid^2}$$

and

$$\psi_s^{(2)} = -\frac{\gamma_\rho\psi_i}{\mid \psi_i \mid^2}\left(1 + \frac{\gamma_\rho}{\mid \psi_i \mid^2}\right)$$

respectively. Thus, with

$$S(\mathbf{r},\omega) = R(\mathbf{r})H(\omega)F(\omega)$$

where

$$F(\omega) = \int_{-\infty}^{\infty} f(t)\exp(-i\omega t)dt$$

and $f(t)$ is given by equation (14), the solution for $\Psi_s^{(1)}$ becomes

$$\Psi_s^{(1)}(\mathbf{r},t) = \frac{\gamma_\rho(\mathbf{r})}{R(\mathbf{r})}\frac{1}{2\pi}\int_{-\Omega}^{\Omega} \frac{F(\omega)}{\mid F(\omega) \mid^2 + \epsilon} \exp(i\omega t)d\omega \tag{18}$$

where ϵ is a regularising constant.

Figure 10 shows a numerical example of the temporal characteristics associated with this solution for $\epsilon = 10^{-9}$

computed over a 1000 element array. The spectrum $F(\omega)$ is computed from the source function $f(t)$ given by equation (14) for $\gamma = 1.55$ using MARLAB (V7) *rand*, *seed* $= 1$ and normalisation condition $\|f(t)\|_\infty = 1$. The figure compares this result with the signal

$$\bar{f}(t) = \frac{1}{2\pi}\int_{-\Omega}^{\Omega} F(\omega)\exp(i\omega t)d\omega$$

used to 'source' the solution.

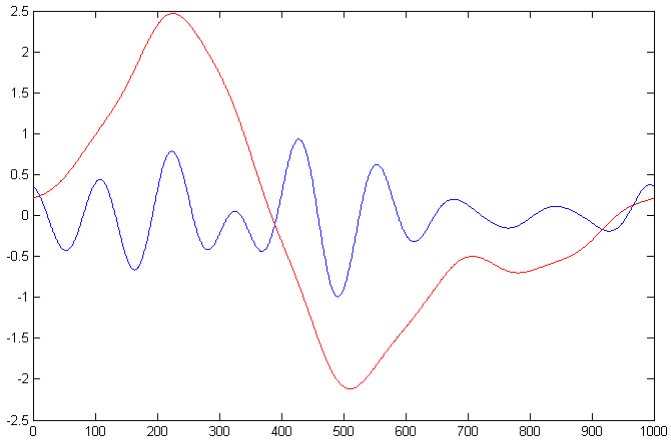

Figure 10: Time dependent component of the function $\Psi_s(\mathbf{r},t)$ given by equation (18) for $\Omega = 10$ (Red) and the normalised source function $\bar{f}(t)$ (Blue).

This example illustrates the ability for a low spatial frequency and phase only scattering model to generate large amplitude waves even when the scattering function is a constant. This is due to the phase only solution being characterised by the inverse filter $F^*/\mid F\mid^2$. In contrast, if the phase only condition is relaxed, then the first and second order scattered fields become

$$\psi_s^{(1)} = -\gamma_\rho\psi_i$$

and

$$\psi_s^{(2)} = -\gamma_\rho(1-\gamma_\rho)^2\psi_i - \gamma_\rho^2\psi_i$$

respectively, and, for constant γ_ρ, the temporal characteristics of both solutions are characterised by $F(\omega)$. This approach to modelling freak waves is similar to modelling the scattering of electromagnetic waves from a random fractal surface [45] but relies on a low frequency condition to derive equation (18).

8 Conclusion

The model presented in this paper provides a 'route to unification' between linear and nonlinear models for modelling deep water surface waves. Based on generalizing the cubic nonlinear Schrödinger equation to

$$\left(\nabla^2 + i^q\partial_t^q\right)\Psi(\mathbf{r},t) = -\kappa\mid\Psi(\mathbf{r},t)\mid^2\Psi(\mathbf{r},t) - s(\mathbf{r},t)$$

with

$$q\in[1,2],\quad \kappa = (2-q)$$

and considering separable forms for $\Psi(\mathbf{r},t)$ and $s(\mathbf{r},t)$ given by $\Psi(\mathbf{r},t) = \phi(\mathbf{r})u(t)$ and $s(\mathbf{r},t) = R(\mathbf{r})f(t)$, respectively, we have obtained the Green's function transformation (ignoring scaling constants)

$$u(t)\nabla^2\phi(\mathbf{r}) = \mathrm{sinc}(\Omega t)\otimes_t f(t)R(\mathbf{r})$$

$$+\kappa\mathrm{sinc}(\Omega t)\otimes_t\mid u(t)\mid^2 u(t)\mid\phi(\mathbf{r})\mid^2\phi(\mathbf{r})$$

where Ω is the bandwidth of the wavefield. Crucially, this result is based on considering a low bandwidth condition in which $\Omega\to 0$ that, compared with other applications, can be applied in the case of modelling low frequency sea waves.

The models for $f(t)$ and $R(\mathbf{r})$ are both based on self-affine stochastic functions, i.e.

$$f(t) = \frac{1}{\Gamma(1/\gamma)t^{1-1/\gamma}}\otimes_t d_t n(t),\quad n(t)\in[0,1],\quad \Pr[n(t)] = 1$$

where γ is the Lévy index and

$$R(\mathbf{r}) = \frac{\exp(-k_0\hat{\mathbf{n}}\cdot\mathbf{r})}{r^{2-q}}\otimes_{\mathbf{r}}\nabla^p n(\mathbf{r}),\quad q>p,$$

$$\Pr[n(\mathbf{r})] = \mathrm{Gauss}(x)$$

We have developed a model for wind velocities based on the application of a Lévy distributed field obtained from an analysis of experimental data. This has shown that wind velocities are statistically self-affine. Thus, we may conclude that the conversion of wind energy into wave energy is self-affine. Moreover, the force generated through the rate of change of wind velocity is not a Gaussian process but, a Lévy process in which extreme values are more common. This is typical of many naturally occurring [42] and man-made time series. An important example of the latter case includes financial time series, e.g. [43] and [44].

The model developed depends on this non-Gaussian stochasticism in which Ω defines the bandwidth at which wind energy is converted into wave energy. The fact that wind forces are non-Gaussian may, according to the model presented, account for the more common occurrence of freak waves than would be expected for Gaussian processes alone.

Although the cubic NLS equation for modelling freak waves forms a central theme of this paper, we have also

considered a low spatial frequency scattering model to illustrate that there are other 'routes' to freak wave modelling. Under the phase only condition, this approach reveals that the time-dependent characteristics of the scattered wave are determined by the inverse of the spectrum of the source function which is independent of the scattering function.

Unlike phenomenological models such as the (cubic) NLS equation, the scattering model considered in Section 7 is based on the Navier-Stokes equations. In order to illustrate the solution method considered and some of its characteristics, we have considered a wave equation for the scalar velocity field propagating through a non-viscous fluid where the relaxation time is zero. Thus, a further development will be to consider a model for wave propagation and scattering in a homogeneous viscous fluid.

Appendix A: Generalized Fourier Transform of $\mid \mathbf{r} \mid^q$ for $\mathbf{r} \in \mathbb{R}^n$

Theorem. If $q \neq 2m$ or $-n-2m$ where $m = 0, 1, 2, ...,$ then

$$\int_{-\infty}^{\infty} r^q \exp(-i\mathbf{k}\cdot\mathbf{r}) d^n\mathbf{r} = \frac{(\frac{1}{2}q+\frac{1}{2}n-1)!}{(-\frac{1}{2}q-1)!} 2^{q+n}\pi^{n/2}k^{-q-n}$$

where $\mathbf{k}$ and $\mathbf{r}$ are the n-dimensional vectors $(k_1, k_2, ..., k_n)$ and $(r_1, r_2, ..., r_n)$ respectively,

$$r \equiv \mid \mathbf{r} \mid = \sqrt{r_1^2 + r_2^2 + ... + r_n^2},$$

$$k \equiv \mid \mathbf{k} \mid = \sqrt{k_1^2 + k_2^2 + ... + k_n^2}$$

and

$$\int_{-\infty}^{\infty} f(\mathbf{r}) \exp(-i\mathbf{k}\cdot\mathbf{r}) d^n\mathbf{r}$$

is taken to mean

$$\int_{-\infty}^{\infty}\int_{-\infty}^{\infty}...\int_{-\infty}^{\infty} f(r_1, r_2, ..., r_n) \exp[-i(k_1r_1+k_2r_2+...+k_nr_n)]$$

$$dr_1 dr_2 ..., dr_n$$

Proof. The proof of this result is based two results:

(i) If f is a function of r only, then

$$F(\mathbf{k}) = \left(1 - \frac{\partial^2}{\partial k_1^2} - \frac{\partial^2}{\partial k_2^2} - ... - \frac{\partial^2}{\partial k_n^2}\right)^N$$

$$\times (2\pi)^{n/2} \int_0^{\infty} \frac{f(r) r^{n-1}}{(1+r^2)^N} \frac{J_{\frac{n-2}{2}}(kr)}{(kr)^{(n/2)-1}} dr$$

where N is a positive integer and $J_{(n-2)/2}$ is the Bessel function (of order $(n-2)/2$).

(ii) For Bessel Functions,

$$\frac{(2\pi)^{n/2}}{k^{(n/2)-1}} \int_0^{\infty} \frac{r^{q+(n/2)}}{(1+r^2)^N} J_{\frac{n-2}{2}}(kr) dr$$

$$= \frac{\pi^{n/2}(\frac{1}{2}q+\frac{1}{2}n-1)!(N-\frac{1}{2}q-\frac{1}{2}n-1)!}{(N-1)!(\frac{1}{2}n-1)!}$$

$$\times {}_1F_2(\tfrac{1}{2}q+\tfrac{1}{2}n; \tfrac{1}{2}q+\tfrac{1}{2}n-N+1, \tfrac{1}{2}n; \tfrac{1}{4}k^2)$$

$$+ \frac{\pi^{n/2}k^{2N-q-n}(\frac{1}{2}q+\frac{1}{2}n-N-1)!}{(N-\frac{1}{2}q-1)!2^{2N-q-n}}$$

$$\times {}_1F_2(N; N-\tfrac{1}{2}q, N+1-\tfrac{1}{2}q-\tfrac{1}{2}n; \tfrac{1}{4}k^2) \qquad (A.1)$$

where

$${}_1F_2(a; b, c; x) = 1 + \frac{a}{1!bc}x + \frac{a(a+1)}{2!b(b+1)c(c+1)}x^2 + ...$$

The first of these results can be obtained by choosing a polar axis to lie along the direction of $\mathbf{k}$ so that $\mathbf{k}\cdot\mathbf{r} = kr\cos\theta_1$ and

$$F(\mathbf{k}) = \int_{-\infty}^{\infty} f(r) \exp(-i\mathbf{k}\cdot\mathbf{r}) d\mathbf{r}$$

$$= \int_0^{\infty} f(r) r^{n-1} \int_0^{\pi} \exp(-ikr\cos\theta_1) \sin^{n-2}\theta_1 d\theta_1$$

$$\times \int_0^{\pi} ... \int_0^{2\pi} \sin^{n-3}\theta_2 ... \sin\theta_{n-2} d\theta_2 ... d\theta_{n-1} dr$$

$$= \int_0^{\infty} f(r) r^{n-1} \frac{2\pi^{(n-1)/2}}{(\frac{1}{2}n-\frac{3}{2})!}$$

$$\times \int_0^{\pi} \exp(-ikr\cos\theta_1) \sin^{n-2}\theta_1 d\theta_1 dr$$

using

$$\int_0^{\pi} \sin^{\nu} d\theta = \frac{(\frac{1}{2}\nu-\frac{1}{2})!\pi^{1/2}}{(\frac{1}{2}\nu)!}.$$

Now,

$$-\left(\frac{\partial^2}{\partial k_1^2} + \frac{\partial^2}{\partial k_2^2} + ... + \frac{\partial^2}{\partial k_n^2}\right)$$

$$= \int_{-\infty}^{\infty} f(r)(r_1^2 + r_2^2 + ... + r_n^2) \exp(-i\mathbf{k}\cdot\mathbf{r}) d^n\mathbf{r}$$

and therefore

$$\left(1-\frac{\partial^2}{\partial k_1^2}-\frac{\partial^2}{\partial k_2^2}-...-\frac{\partial^2}{\partial k_n^2}\right)^N$$

$$=\int_{-\infty}^{\infty} f(r)(1+r^2)^N \exp(-i\mathbf{k}\cdot\mathbf{r})d^n\mathbf{r}.$$

Hence, we can write

$$F(\mathbf{k})=\left(1-\frac{\partial^2}{\partial k_1^2}+\frac{\partial^2}{\partial k_2^2}-...-\frac{\partial^2}{\partial k_n^2}\right)^N$$

$$\times(2\pi)^{n/2}\int_0^{\infty}\frac{f(r)r^{n-1}}{(1+r^2)^N}\frac{J_{\frac{n-2}{2}}(kr)}{(kr)^{(n/2)-1}}dr. \qquad (A.2)$$

The ratio of two successive terms u_{n+1}/u_n in the infinite series for ${}_1F_2$ is $(a+n)x/[(n+1)(b+n)(c+n)]$ which tends to zero as $n\to\infty$ for any finite x. Thus, the series for ${}_1F_2$ converges absolutely and uniformly with respect to x and the same is true of its derivatives (provided that neither b or c is a negative integer or zero when the series diverges). Therefore,

$$\left(\frac{\partial^2}{\partial k_1^2}+\frac{\partial^2}{\partial k_2^2}+...+\frac{\partial^2}{\partial k_n^2}\right){}_1F_2(a;b,\tfrac{1}{2}n;\tfrac{1}{4}k^2)$$

$$=\frac{(b-1)!(\frac{1}{2}-1)!}{(a-1)!}\left(\frac{\partial^2}{\partial k_1^2}+\frac{\partial^2}{\partial k_2^2}+...+\frac{\partial^2}{\partial k_n^2}\right)$$

$$\times\sum_{s=0}^{\infty}\frac{(a+s-1)!(\frac{1}{2}k)^{2s}}{(b+s-1)!(\frac{1}{2}n+s-1)!s!}$$

$$=\frac{(b-1)!(\frac{1}{2}n-1)!}{(a-1)!}\sum_{s=0}^{\infty}\frac{(a+s-1)!(\frac{1}{2}k)^{2s-2}}{(b+s-1)!(\frac{1}{2}n+s-2)!(s-1)!}.$$

The term for $s=0$ disappears so that, by replacing s by $s+1$ we obtain

$$\left(\frac{\partial^2}{\partial k_1^2}+\frac{\partial^2}{\partial k_2^2}+...+\frac{\partial^2}{\partial k_n^2}-1\right){}_1F_2(a;b,\tfrac{1}{2}n;\tfrac{1}{4}k^2)$$

$$=\frac{(b-1)!(\frac{1}{2}n-1)!}{(a-1)!}\sum_{s=0}^{\infty}\frac{(a+s-1)!(\frac{1}{2}k)^{2s}}{(b+s)!(\frac{1}{2}n+s-1)!s!}(a+s-b-s)$$

$$=\frac{a-b}{b}{}_1F_2(a;b+1,\tfrac{1}{2}n;\tfrac{1}{4}k^2).$$

Hence,

$$\left(\frac{\partial^2}{\partial k_1^2}+\frac{\partial^2}{\partial k_2^2}+...+\frac{\partial^2}{\partial k_n^2}-1\right)^N{}_1F_2(a;b,\tfrac{1}{2}n;\tfrac{1}{4}k^2)$$

$$=\frac{(a-b)(a-b-1)...(a-b-N+1)}{b(b+1)...(b+N-1)}$$

$$\times{}_1F_2(a;b+N,\tfrac{1}{2}n;\tfrac{1}{4}k^2). \qquad (A.3)$$

In the first term of (A.1) $a=\frac{1}{2}(q+n), b=\frac{1}{2}(q+n)-N+1$ so that $a-b=N+1$ with the result that the right hand side of the equation vanishes. For the second term of (A.1), consider, with $b>0$

$$\left(\frac{\partial^2}{\partial k_1^2}+\frac{\partial^2}{\partial k_2^2}+...+\frac{\partial^2}{\partial k_n^2}\right)k^{2b}{}_1F_2(a;b+\tfrac{1}{2}n,b+1;\tfrac{1}{4}k^2)$$

$$=\frac{(b+\frac{1}{2}n-1)!b!}{(a-1)!}\sum_{s=0}^{\infty}\frac{(a+s-1)!k^{2b+2s-2}}{4^{s-1}(b+\frac{1}{2}n-2+s)!(b+s-1)!s!}$$

as above. Hence,

$$\left(\frac{\partial^2}{\partial k_1^2}+\frac{\partial^2}{\partial k_2^2}+...+\frac{\partial^2}{\partial k_n^2}-1\right)k^{2b}{}_1F_2(a;b+\tfrac{1}{2}n,b+1;\tfrac{1}{4}k^2)$$

$$=\frac{(b+\frac{1}{2}n-1)!b!}{(a-1)!}\Big[\frac{(a-1)!4k^{2b-2}}{(b+\frac{1}{2}n-2)!(b-1)!}$$

$$+\sum_{s=0}^{\infty}\frac{(a+s-2)!(a-1)k^{2b+2s-2}}{4^{s-1}(b+\frac{1}{2}n-2+s)!(b+s-1)!s!}\Big]$$

from which it is evident that

$$\left(\frac{\partial^2}{\partial k_1^2}+\frac{\partial^2}{\partial k_2^2}+...+\frac{\partial^2}{\partial k_n^2}-1\right)k^{2b}$$

$$\times{}_1F_2(1;b+\tfrac{1}{2}n,b+1;\tfrac{1}{4}k^2)$$

$$=(b+\tfrac{1}{2}n-1)4bk^{2b-2} \qquad (A.4)$$

and

$$\left(\frac{\partial^2}{\partial k_1^2}+\frac{\partial^2}{\partial k_2^2}+...+\frac{\partial^2}{\partial k_n^2}-1\right)k^{2b}$$

$$\times{}_1F_2(a;b+\tfrac{1}{2}n,b+1;\tfrac{1}{4}k^2)$$

$$=4b(b+\tfrac{1}{2}n-1)k^{2b-2}{}_1F_2(a-1;b+\tfrac{1}{2}n-1,b;\tfrac{1}{4}k^2),$$

$$a\neq 1$$

Consequently, if $a\neq 1$ or 2, then since

$$\left(\frac{\partial^2}{\partial k_1^2}+\frac{\partial^2}{\partial k_2^2}+...+\frac{\partial^2}{\partial k_n^2}\right)k^q=q(q+n-2)k^{q-2}$$

for all q except those for which

$$q+n=2,0,-2,-4,...$$

if follows that

$$\left(\frac{\partial^2}{\partial k_1^2}+\frac{\partial^2}{\partial k_2^2}+...+\frac{\partial^2}{\partial k_n^2}-1\right)k^{2b}$$

$$\times{}_1F_2(a;b+\tfrac{1}{2}n,b+1;\tfrac{1}{4}k^2)$$

$$=4^2b(b-1)(b+\tfrac{1}{2}n-1)(b+\tfrac{1}{2}n-2)k^{2b-4}$$

$$\times{}_1F_2(a-2;b+\tfrac{1}{2}n-2,b-1;\tfrac{1}{4}k^2)$$

where, in deriving this result, since it cannot be assumed that $b-1>0$, with $b=N-\frac{1}{2}q-\frac{1}{2}n$ we impose the condition $q=2m\ \ (m=0,1,2,...)$. Thus, using (A.4) we can write

$$\left(\frac{\partial^2}{\partial k_1^2}+\frac{\partial^2}{\partial k_2^2}+...+\frac{\partial^2}{\partial k_n^2}-1\right)^N k^{2N-q-n}$$

$$\times {}_1F_2(N;N-\tfrac{1}{2}q,N+1-\tfrac{1}{2}q-\tfrac{1}{2}n;\tfrac{1}{4}k^2)$$

$$=\left(\frac{\partial^2}{\partial k_1^2}+\frac{\partial^2}{\partial k_2^2}+...+\frac{\partial^2}{\partial k_n^2}-1\right)$$

$$\times 4^{N-1}\frac{(N-\frac{1}{2}q-\frac{1}{2}n)!(N-\frac{1}{2}q-1)!k^{-q-n+2}}{(-\frac{1}{2}q-\frac{1}{2}n+1)!(-\frac{1}{2}q)!}$$

$$\times {}_1F_2(1;-\tfrac{1}{2}q+1,-\tfrac{1}{2}q-\tfrac{1}{2}n+2;\tfrac{1}{4}k^2)$$

$$=\frac{(N-\frac{1}{2}q-\frac{1}{2}n)!(N-\frac{1}{2}q-1)!4^N k^{-q-n}}{(-\frac{1}{2}q-\frac{1}{2}n)!(-\frac{1}{2}q-1)!}. \qquad (A.5)$$

Using equations (A.5) and (A.3) in equations (A.1) and (A.2) we find that

$$F(\mathbf{k})=\frac{(N-\frac{1}{2}q-\frac{1}{2}n)!(\frac{1}{2}q+\frac{1}{2}n-N-1)!}{(-\frac{1}{2}q-\frac{1}{2}n)!(-\frac{1}{2}q-1)!}$$

$$\times 2^{q+n}(-1)^N\pi^{n/2}k^{-q-n}.$$

Finally, using the formula

$$z!(-z)!=\frac{\pi z}{\sin\pi z}$$

we have

$$(N-\tfrac{1}{2}q-\tfrac{1}{2}n)!(\tfrac{1}{2}q+\tfrac{1}{2}n-N-1)!$$

$$=\frac{\pi}{\sin\pi(\frac{1}{2}q+\frac{1}{2}n-N)}$$

$$=\frac{(-1)^N\pi}{\sin\frac{1}{2}\pi(q+n)}=(\tfrac{1}{2}q+\tfrac{1}{2}n-1)!(-\tfrac{1}{2}q-\tfrac{1}{2}n)!(-1)^N$$

so that

$$F(\mathbf{k})=\frac{(\frac{1}{2}q+\frac{1}{2}n-1)!}{(-\frac{1}{2}q-1)!}2^{q+n}\pi^{n/2}k^{-q-n}.$$

We can write this result using the Gamma function notation where

$$m!=\Gamma(m+1)=\int_0^\infty t^m\exp(-pt)dt$$

Thus,

$$F(\mathbf{k})=\frac{\Gamma\left(\frac{q+n}{2}\right)}{\Gamma\left(-\frac{q}{2}\right)}2^{q+n}\pi^{n/2}k^{-q-n}$$

Appendix B: Condition for Convergence of the Iterative Solution to Equation (11)

Theorem. The condition for the convergence of the iterative solution to (11) is that

$$\|u(t)\|_2^2<\frac{1}{3\kappa}\sqrt{\frac{\pi}{\Omega}}$$

Proof. Consider the error function at the n^{th} iteration to be ϵ_n so that at the n^{th} order iteration can be considered to be given by $u_n(t)=u(t)+\epsilon_n(t)$ where $u(t)$ is the exact solution. The iterative solution to (11), then becomes

$$u(t)+\epsilon_{n+1}(t)=\frac{\Omega}{\pi}\text{sinc}(\Omega t)\otimes_t f(t)$$

$$+\frac{\kappa\Omega}{\pi}\text{sinc}(\Omega t)\otimes_t[u(t)+\epsilon_n(t)]\mid u(t)+\epsilon_n(t)\mid^2$$

Expanding the nonlinear term we obtain

$$\epsilon_{n+1}=\frac{\kappa\Omega}{\pi}\text{sinc}(\Omega t)\otimes_t[u^2(t)\epsilon_n^*(t)+2\epsilon(t)\mid u(t)\mid^2$$

$$+2u(t)\mid\epsilon_n(t)\mid^2+\epsilon^2(t)u^*(t)+\mid\epsilon_n(t)\mid^2\epsilon_n(t)$$

Taking the norm of this equation, and noting that for two piecewise continuous functions $f(t)$ and $g(t)$,

$$\|f(t)\otimes_t g(t)\|\le\|f(t)\|\times\|g(t)\|,$$

$$\|f(t)g(t)\|\le\|f(t)\|\times\|g(t)\|$$

and

$$\|f^n(t)\|\le\|f(t)\|^n,$$

we obtain

$$\|\epsilon_{n+1}\|\le\frac{\kappa\Omega}{\pi}\|\text{sinc}(\Omega t)\|$$

$$\times[\|u(t)\|^2\times\|\epsilon_n(t)\|+3\|u(t)\|\times\|\epsilon_n(t)\|^2+\|\epsilon_n(t)\|^3]$$

For convergence, we must have

$$\lim_{n\to\infty}\|\epsilon_n\|=0$$

from which it follows that

$$\frac{\|\epsilon_{n+1}(t)\|}{\|\epsilon_n(t)\|}\le\frac{\kappa\Omega}{\pi}\|\text{sinc}(\Omega t)\|\times\|u(t)\|^2$$

Thus, since

$$\lim_{n\to\infty}\left(\frac{\|\epsilon_{n+1}\|}{\|\epsilon_n\|}\right)=1$$

we may consider the following condition for convergence:

$$\frac{\kappa\Omega}{\pi}\|\text{sinc}(\Omega t)\|\times\|u(t)\|^2<1$$

Using an ℓ_2 (Euclidean) norm and noting that

$$\int_{-\infty}^{\infty} \mathrm{sinc}^2(x)dx = \pi$$

the convergence condition becomes

$$\|u(t)\|_2^2 < \frac{1}{3\kappa}\sqrt{\frac{\pi}{\Omega}}$$

Appendix C: Condition for Convergence of the Iterative Solution to Equation (15)

Theorem. The condition for the convergence of (15) is that

$$\|\phi(\mathbf{r})\| < \left(\frac{2}{9\pi\kappa^2}\right)^{\frac{1}{4}}, \quad r \in [0,1]$$

Proof. From (15)

$$\phi(\mathbf{r}) + \epsilon_{n+1}(\mathbf{r}) = -\ln(r) \otimes_{\mathbf{r}} R(\mathbf{r})$$

$$-\kappa \ln(r) \otimes_{\mathbf{r}} \mid \phi(\mathbf{r}) + \epsilon_n(\mathbf{r}) \mid^2 [\phi(\mathbf{r}) + \epsilon_n(\mathbf{r})]$$

Expanding the nonlinear term and taking norms, we obtain

$$\frac{\|\epsilon_{n+1}(\mathbf{r})\|}{\|\epsilon_n(\mathbf{r})\|} \leq 3\kappa \| \ln(r) \| \|\phi(\mathbf{r})\|^2$$

so that as $n \to \infty$ we require that

$$3\kappa \| \ln r \| \|\phi(\mathbf{r})\|^2 < 1$$

For $r \in [0,1]$

$$\| \ln r \|_2 = \left(\int_0^{2\pi} \int_0^1 [\ln(r)]^2 r dr d\theta \right)^{\frac{1}{2}}$$

and using the result (for independent variable x)

$$\int_0^1 x^m (\ln x)^n dx = \frac{(-1)^n m!}{(m+1)^{n+1}}$$

we obtain

$$\| \ln r \| = \sqrt{\frac{\pi}{2}}$$

from which the condition is derived.

Appendix D: Derivation of the Wave Equation from the Linearised Navier Stokes Equations

9 Derivation of the Wave Equation

The wave equation is obtained by linearising the hydrodynamic equations of motion (the Navier-Stokes equations) and may be written in the form

$$\nabla \cdot \mathbf{v} = \kappa \frac{\partial p}{\partial t} \tag{D.1}$$

$$\nabla p = \rho \frac{\partial \mathbf{v}}{\partial t} - \nabla \cdot \mathbf{T} \tag{D.2}$$

where $\mathbf{v}(\mathbf{r},t)$ is the velocity field (length/time), $p(\mathbf{r},t)$ is the pressure field (force/area), $\mathbf{T}(\mathbf{r},t)$ is the material stress tensor (force/volume), $\rho(\mathbf{r})$ is the density (mass/volume) and $\kappa(\mathbf{r})$ is the compressibility (area/force). It is assumed that the material to which these equations comply is adiabatic. The first equation comes from the law of conservation of mass and the second equation is a consequence of the law of conservation of momentum. For compression waves alone, the material stress tensor is given by

$$\mathbf{T} = \mathbf{I}\alpha \nabla \cdot \mathbf{v} + 2\beta \nabla \mathbf{v}$$

where $\mathbf{I}$ is the unit dyad. The parameters α and β are related to the bulk ζ and shear η viscosities of a material by the equations

$$\alpha = \zeta - \frac{2}{3}\eta \quad \text{and} \quad \beta = \eta$$

It is assumed that ρ, κ, α and β are both isotropic and time invariant and by decoupling equations (D.1) and (D.2) for p we obtain

$$\nabla \left(\frac{1}{\kappa} \nabla \cdot \mathbf{v} \right) = \rho \frac{\partial^2 \mathbf{v}}{\partial t^2} - \frac{\partial}{\partial t} \left[\nabla(\alpha \nabla \cdot \mathbf{v}) + 2\nabla \cdot (\beta \nabla \mathbf{v}) \right] \tag{D.3}$$

By adding

$$\frac{\partial}{\partial t}[\nabla(\alpha_0 \nabla \cdot \mathbf{v}) + 2\nabla \cdot (\beta_0 \nabla \mathbf{v})] - \rho_0 \frac{\partial^2 \mathbf{v}}{\partial t^2} - \nabla \left(\frac{1}{\kappa_0} \nabla \cdot \mathbf{v} \right)$$

to both sides of equation (D.3) where ρ_0, κ_0, α_0 and β_0 are constants and noting that, for compression waves only, $\nabla \times \mathbf{v} = 0$ so that

$$\nabla \times \nabla \times \mathbf{v} = -\nabla^2 \mathbf{v} + \nabla(\nabla \cdot \mathbf{v}) = 0$$

or

$$\nabla(\nabla \cdot \mathbf{v}) = \nabla^2 \mathbf{v}$$

we obtain the wave equation

$$\left(1 + \tau_0 \frac{\partial}{\partial t}\right) \nabla^2 \mathbf{v} - \frac{1}{c_0^2} \frac{\partial^2 \mathbf{v}}{\partial t^2} = \gamma_\rho \frac{1}{c_0^2} \frac{\partial^2 \mathbf{v}}{\partial t^2} + \nabla(\gamma_\kappa \nabla \cdot \mathbf{v})$$

$$-\tau\frac{\partial}{\partial t}\left(\nabla(\gamma_\alpha\nabla\cdot\mathbf{v})+2\nabla\cdot(\gamma_\beta\nabla\mathbf{v})\right)$$

where

$$\gamma_\kappa=\frac{\kappa-\kappa_0}{\kappa},\quad \gamma_\rho=\frac{\rho-\rho_0}{\rho_0},\quad \gamma_\alpha=\frac{\alpha-\alpha_0}{\alpha_0+2\beta_0}$$

$$\gamma_\beta=\frac{\beta-\beta_0}{\alpha_0+2\beta_0},\quad c_0=\frac{1}{\sqrt{\rho_0\kappa_0}}\quad\text{and}\quad \tau_0=\kappa_0(\alpha_0+2\beta_0).$$

The parameter τ_0 is known as the relaxation time and may be written in the form

$$\tau_0=\frac{\alpha_0+2\beta_0}{\rho_0 c_0^2}$$

The quantity $\alpha_0+2\beta_0=\zeta_0+4\eta_0/3$ is the compressional viscosity. If $\kappa=\kappa_0$, $\alpha=\alpha_0$, $\beta=\beta_0$, any vector component of the velocity Ψ say, can be taken to conform to the wave equation

$$\left(1+\tau_0\frac{\partial}{\partial t}\right)\nabla^2\Psi-\frac{1}{c_0^2}\frac{\partial^2\Psi}{\partial t^2}=\gamma_\rho\frac{1}{c_0^2}\frac{\partial^2\Psi}{\partial t^2}$$

Thus, for $\tau_0=0$ and with

$$\Psi(\mathbf{r},t)=\frac{1}{(2\pi)^3}\int_{-\infty}^{\infty}\psi(\mathbf{r},\omega)\exp(i\omega t)d\omega$$

we obtain

$$\left(\nabla^2+k^2\right)\psi(\mathbf{r},\omega)=-k^2\gamma(\mathbf{r})\psi(\mathbf{r},\omega)$$

where $k=\omega/c_0$.

Acknowledgments

The author is supported by the Science Foundation Ireland Stokes Professorship Programme. The author gratefully acknowledges Mr Keith Sunderland, School of Electrical Engineering Systems, Dublin Institute of Technology for supplying the wind velocity data presented in Section 5.

References

[1] Bretschneider, C., "The Generation and Decay of Wind Waves in Deep Water", Trans. Am. Geophys. Union, vol. 33, pp. 381-389, 1952

[2] Pierson, W. and Moskowitz, L. "A Proposed Spectral Form for Fully Developed Wind Seas based on the Similarity Theory of S.A. Kitaigorodskii", J. Geophys. Res., Vol. 69, pp. 5181-5190, 1964

[3] Broad, W. J., "Rogue Giants at Sea", The New Yor Times, 2006; http://www.nytimes.com/2006/07/11/science/11wave.html

[4] Physics Daily, "Freak Waves", The Physics Encyclopedia http://www.physicsdaily.com/physics/Freak_wave

[5] Lavrenova, I. V. and Porubov, A. V., "Three reasons for freak wave generation in the non-uniform current" European Journal of Mechanics - B/Fluids, Vol. 25, Issue 5, pp. 574-585, 2006

[6] Lopatoukhin, L. J. and Boukhanovsky, A. V., "Freak Wave Generation and their Probability", *International Shipbuilding Progress*, IOS Press, Vol. 51, No. 2-3, pp. 157-171, 2006.

[7] W. Dick, W. *Wave Energy Converter*, US Patent No. 6857266, 2005.

[8] Eidsmoen, H., *Theory and Simulation of Heaving-buoy Wave-energy Converters with Control*, Ph.D. Dissertation, Norwegian University of Science and Technology, 1995.

[9] Callaghan, J., *Future Marine Energy*, The Carbon Trust, 2003.

[10] AWS Ocean Energy Ltd., *AWS Technology*, http://www.waveswing.com/

[11] Draupner Monster Wave http://www.youtube.com/watch?v=K_JOBOvJEOg

[12] Draupner Wave, http://en.wikipedia.org/wiki/Draupner_wave

[13] Sulem, C and Sulem, P. L., *The Nonlinear Schrdinger Equation: Self Focusing and Wave Collapse*, Springer, 1999

[14] Nassar, A. B., Bassalo, J. M. F., Alencar, P. T. S., De Souza, J. F, De Oliveira, J. E. and Cattani, M., " Gaussian Solitons in Nonlinear Schrödinger Equation", *Il Nuovo Cimento*, Vol. 117B, No. 8, pp. 941-946, 2002

[15] Bartsch, T. and Wang Z. Q., "Sign Changes Solutions of Nonloinear Schrödinger Equations", *Topologocal Methods in Nonlinear Analysis*, Journal of the Schauder Center, Vol. 13, pp. 191-198, 1999

[16] Ulmer, W., "A Solution Spectrum of the Nonlinear Schrödinger Equation", International Journal of Theoretical Physics, Vol. 28, No. 5, pp. 527-542, 1989

[17] Shukla, P. K., Kourakis, I., Eliasson, B., Markland, M. and Stenflo, L., "Instability and Evolution of Nonlinearly Interacting Water Waves", Phys. Rev. Lett. 96, 094501, 2006

[18] Eliasson, B. and Shukla, P. K., "Instability and Nonlinear Evolution of Narrow-band Directional Ocean Waves", Phys. Rev. Lett. 105, 014501, 2010

[19] Zakharov, V. E. and Schulman, E. I., "Degenerated Dispersion Laws, Motion Invariant and Kinetic Equations", Physica, 1D, pp. 185-250, 1980

[20] Bronski, J. C., Carr, L. D., Deconinck, B. and Kutz, J. N., "Bose-Einstein Condensates in Standing Waves: The Cubic Nonlinear Schrödinger Equation with a Periodic Potential", Phys. Rev. Lett. Vol. 86, No. 8, pp. 1402-1405, 2001.

[21] Zakharov, V. E. and Shabat, A. B., "Exact Theory of Two-Dimensional Self-Focusing and One-Dimensional Self-Modulation of Waves in Nonlinear Media", Soviet Physics, JETP, Vol. 34, pp. 62-69, 1972

[22] Y C Ma, Y. C., "The Perturbed Plane-wave Solutions of the Cubic Schroedinger Equation", Studies in Applied Mathematics, Vol. 60, pp. 43-58, 1979

[23] Dysthe, K. B. and Trulsen, K., "Note of Breather Type Solutions of the NLS Equation as a Model for Freak Waves", Phys. Scripta T82, pp 48-52, 1999.

[24] Peregrine, D. H., "Water Waves, Nonlinear Schrödinger Equations and their Solutions", J. Austral. Math. Soc. Series B 25 (1983), pp. 1643, 1983

[25] Lvov, V. *Fundamentals of Nonlinear Physics* http://lvov.weizmann.ac.il/Course/FreakWaves.pdf

[26] Henderson, K. L., Peregrine, D. H. and Dold, J. W., "Unsteady Water Wave Modulations: Fully Nonlinear Solutions and Comparison with the NLS Equation, Wave Motion, Vol. 29, 341-361, 1999.

[27] Zakharov, V. E., "Stability of Periodic Waves of Finite Amplitude on the Surface of a Deep Fluid". Journal of Applied Mechanics and Technical Physics 9(2), pp. 190194, 1968

[28] Dyachenko, A. I. and Zakharov, V. E., "On the Formation of Freak Waves on the Surface of Deep Water", JETP Letters, pp. 307-311, 2009

[29] Barndorff-Nielsen, O. E., Mikosch and Resnick, S. I. (Eds.), *Lévy Processes: Theory and Applications*, Birkhauser, 2001

[30] Applebaum, D. *Lévy Processes and Stochastic Calculus*, Cambridge University Press, 2004

[31] Shlesinger, M. F., Zaslavsky, G. M. and Frisch U. (Eds.), *Lévy Flights and Related Topics in Physics*, Springer 1994.

[32] Nonnenmacher T. F., "Fractional Integral and Differential Equations for a Class of Lévy-type Probability Densities", *J. Phys. A: Math. Gen.*, Vol. 23, pp. L697S-L700S, 1990.

[33] Bertoin J., *Lévy Processes*, Cambridge University Press, 1998

[34] Abea, S. and Thurnerb, S., "Anomalous Diffusion in View of Einsteins 1905 Theory of Brownian Motion", *Physica*, A(356), Elsevier, pp. 403-407, 2005.

[35] Evans, G., Blackledge, J and Yardley, P., *Analytic Methods for Partial Differential Equations*, Springer, 2000.

[36] Berman, S. *Sojourns and Extremes of Stochastic Processes*, CRC Press, 1992

[37] Uhlenbeck, G. E. and Ornstein, L. S. "On the Theory of Brownian Motion", Phys. Rev. Vol. 36, pp. 82341, 1930

[38] Gillespie, D. T., "Exact Numerical Simulation of the OrnsteinUhlenbeck Process and its Integral", Phys. Rev. E, Vol. 54, pp. 208491, 1996

[39] Bibbona, E., Panfilo, G. and Tavella P., "The Ornstein-Uhlenbeck Process as a Model of a Low Pass Filtered White Noise', Metrologia, Vol. 45, pp. S117-S126, 2008

[40] Bivona, S., Bonanno, G., Burlon, R., Gurrera, D. and Leone, C., "Stochastic Models for Wind Speed Forecasting", *Energy Conversion and Management*, Elsevier (Article in Press), 2010

[41] Peszat, S. and Zabczyk, J., *Stochastic Partial Differential Equations with Lévy Noise*, Cambridge University Press, 2007

[42] Kyprianou, A. E., *Introductory Lectures on Fluctuations of Lévy Processes with Applications*, Springer, 2006

[43] Schoutens, W., *Lévy Processes in Finance: Pricing Financial Derivatives*, Wiley, 2003

[44] Blackledge, J. M., "Application of the Fractional Diffusion Equation for Predicting Market Behaviour", IAENG International Journal of Applied Mathematics, Vol. 40, Issue 3, pp. 1-29, 2010 http://www.iaeng.org/IJAM/issues_v40/issue_3/IJAM_40_3_04.pdf

[45] Simonsen, I., Vandembroucq, D. and Roux, S., "Wave Scattering from Self-Affine Surfaces", Phys. Rev. E, Vol. 61, pp. 59145917, 2000.